A narrative review on characterization of acute respiratory distress syndrome in COVID-19-infected lungs using artificial intelligence

S. Suri, Jasjit; Visković, Klaudija...

Journal article, Published version
Rad u časopisu, Objavljena verzija rada (izdavačev PDF)

Permanent link / Trajna poveznica: https://urn.nsk.hr/urn:nbn:hr:184:621996

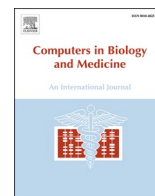*Download date / Datum preuzimanja:* **2025-04-02**

Repository / Repozitorij:

Repository of the University of Rijeka, Faculty of Health Studies - FHSRI Repository

Since January 2020 Elsevier has created a COVID-19 resource centre with free information in English and Mandarin on the novel coronavirus COVID-19. The COVID-19 resource centre is hosted on Elsevier Connect, the company's public news and information website.

A narrative review on characterization of acute respiratory distress syndrome in COVID-19-infected lungs using artificial intelligence

Jasjit S. Suri [a,*], Sushant Agarwal [b,c], Suneet K. Gupta [d], Anudeep Puvvula [a,e], Mainak Biswas [f], Luca Saba [g], Arindam Bit [h], Gopal S. Tandel [i], Mohit Agarwal [d], Anubhav Patrick [j], Gavino Faa [k], Inder M. Singh [a], Ronald Oberleitner [l], Monika Turk [m], Paramjit S. Chadha [a], Amer M. Johri [n], J. Miguel Sanches [o], Narendra N. Khanna [p], Klaudija Viskovic [q], Sophie Mavrogeni [r], John R. Laird [s], Gyan Pareek [t], Martin Miner [u], David W. Sobel [t], Antonella Balestrieri [f], Petros P. Sfikakis [v], George Tsoulfas [w], Athanasios Protogerou [x], Durga Prasanna Misra [y], Vikas Agarwal [z], George D. Kitas [z,aa], Puneet Ahluwalia [ab], Jagjit Teji [ac], Mustafa Al-Maini [ad], Surinder K. Dhanjil [ae], Meyypan Sockalingam [af], Ajit Saxena [p], Andrew Nicolaides [ag], Aditya Sharma [ah], Vijay Rathore [a], Janet N.A. Ajuluchukwu [ai], Mostafa Fatemi [aj], Azra Alizad [ak], Vijay Viswanathan [al], P.K. Krishnan [am], Subbaram Naidu [an]

[a] Stroke Diagnostic and Monitoring Division, AtheroPoint™, Roseville, CA, USA
[b] Advanced Knowledge Engineering Centre, GBTI, Roseville, CA, USA
[c] Department of Computer Science Engineering, PSIT, Kanpur, India
[d] Department of Computer Science Engineering, Bennett University, India
[e] Annu's Hospitals for Skin and Diabetes, Nellore, AP, India
[f] Department of Computer Science Engineering, JIS University, Kolkata, India
[g] Department of Radiology, Azienda Ospedaliero Universitaria, Cagliari, Italy
[h] Department of Biomedical Engineering, NIT, Raipur, India
[i] Department of Computer Science Engineering, VNIT, Nagpur, India
[j] KIET Group of Institutions, Delhi-NCR, India
[k] Department of Pathology - AOU of Cagliari, Italy
[l] Behavior Imaging, Boise, ID, USA
[m] The Hanse-Wissenschaftskolleg Institute for Advanced Study, Delmenhorst, Germany
[n] Department of Medicine, Division of Cardiology, Queen's University, Kingston, Ontario, Canada
[o] Institute of Systems and Robotics, Instituto Superior Tecnico, Lisboa, Portugal
[p] Department of Cardiology, Indraprastha APOLLO Hospitals, New Delhi, India
[q] University Hospital for Infectious Diseases, Zagreb, Croatia
[r] Cardiology Clinic, Onassis Cardiac Surgery Center, Athens, Greece
[s] Heart and Vascular Institute, Adventist Health St. Helena, St Helena, CA, USA
[t] Minimally Invasive Urology Institute, Brown University, Providence, RI, USA
[u] Men's Health Center, Miriam Hospital Providence, Rhode Island, USA
[v] Rheumatology Unit, National Kapodistrian University of Athens, Greece
[w] Aristoteleion University of Thessaloniki, Thessaloniki, Greece
[x] National & Kapodistrian University of Athens, Greece
[y] Sanjay Gandhi Postgraduate Institute of Medical Sciences, Lucknow, UP, India
[z] Academic Affairs, Dudley Group NHS Foundation Trust, Dudley, UK
[aa] Arthritis Research UK Epidemiology Unit, Manchester University, Manchester, UK
[ab] Max Institute of Cancer Care, Max Superspeciality Hospital, New Delhi, India
[ac] Ann and Robert H. Lurie Children's Hospital of Chicago, Chicago, USA
[ad] Allergy, Clinical Immunology and Rheumatology Institute, Toronto, Canada
[ae] AtheroPoint LLC, CA, USA
[af] MV Center of Diabetes, Chennai, India
[ag] Vascular Screening and Diagnostic Centre and University of Nicosia Medical School, Cyprus
[ah] Division of Cardiovascular Medicine, University of Virginia, Charlottesville, VA, USA

* Corresponding author. Institute of Electrical and Electronics Engineers, American Institute of Medical and Biological Engineering, American Insitute of Ultrasound in Medicine, Asia Pacific Vascular Society Stroke Diagnosis and Monitoring Division, AtheroPoint™, Roseville, CA, 95661, USA.
E-mail address: jasjit.suri@atheropoint.com (J.S. Suri).

ai *Department of Medicine, Lagos University Teaching Hospital, Lagos, Nigeria*
aj *Dept. of Physiology & Biomedical Engg., Mayo Clinic College of Medicine and Science, MN, USA*
ak *Dept. of Radiology, Mayo Clinic College of Medicine and Science, MN, USA*
al *MV Hospital for Diabetes and Professor M Viswanathan Diabetes Research Centre, Chennai, India*
am *Neurology Department, Fortis Hospital, Bangalore, India*
an *Electrical Engineering Department, University of Minnesota, Duluth, MN, USA*

ARTICLE INFO

ABSTRACT

COVID-19 has infected 77.4 million people worldwide and has caused 1.7 million fatalities as of December 21, 2020. The primary cause of death due to COVID-19 is Acute Respiratory Distress Syndrome (ARDS). According to the World Health Organization (WHO), people who are at least 60 years old or have comorbidities that have primarily been targeted are at the highest risk from SARS-CoV-2.

Medical imaging provides a non-invasive, touch-free, and relatively safer alternative tool for diagnosis during the current ongoing pandemic. Artificial intelligence (AI) scientists are developing several intelligent computer-aided diagnosis (CAD) tools in multiple imaging modalities, i.e., lung computed tomography (CT), chest X-rays, and lung ultrasounds. These AI tools assist the pulmonary and critical care clinicians through (a) faster detection of the presence of a virus, (b) classifying pneumonia types, and (c) measuring the severity of viral damage in COVID-19-infected patients. Thus, it is of the utmost importance to fully understand the requirements of for a fast and successful, and timely lung scans analysis.

This narrative review first presents the pathological layout of the lungs in the COVID-19 scenario, followed by understanding and then explains the comorbid statistical distributions in the ARDS framework. The novelty of this review is the approach to classifying the AI models as per the by school of thought (SoTs), exhibiting based on segregation of techniques and their characteristics. The study also discusses the identification of AI models and its extension from non-ARDS lungs (pre-COVID-19) to ARDS lungs (post-COVID-19). Furthermore, it also presents AI workflow considerations of for medical imaging modalities in the COVID-19 framework. Finally, clinical AI design considerations will be discussed.

We conclude that the design of the current existing AI models can be improved by considering comorbidity as an independent factor. Furthermore, ARDS post-processing clinical systems must involve include (i) the clinical validation and verification of AI-models, (ii) reliability and stability criteria, and (iii) easily adaptable, and (iv) generalization assessments of AI systems for their use in pulmonary, critical care, and radiological settings.

1. Introduction

In December 2019, the novel coronavirus, severe acute respiratory distress syndrome coronavirus 2 (SARS-CoV-2) [1], appeared in Wuhan, in the Hubei province of the People's Republic of China. The disease caused by the virus was initially called novel coronavirus pneumonia (NCP) by the Chinese government [2]. Even though it has been argued that this disease is syndemic[1] (has both biological and social factors) [3], it was subsequently renamed the coronavirus disease 2019 (COVID-19) by the World Health Organization (WHO). It is currently a global pandemic [4]. It is a respiratory disease that can lead to acute respiratory distress syndrome (ARDS) and eventually to death. As of **December 21, 2020**, more than **77.4 million** COVID-19 cases have been reported, causing **1.7 million** casualties [5]. COVID-19 has a Ro value between 2.43 and 3.10, meaning that it is highly contagious [6]. The colors in Fig. 1 (from white to dark red) show the number of cases reported per million of population worldwide. The eight countries with the highest mortality are the USA, Brazil, India, Mexico, the UK, Italy, France, and Spain [7].

Genetically, COVID-19 is closer to SARS-CoV-1 than to Middle East respiratory syndrome coronavirus (MERS-CoV). However, it differs from SARS-CoV-1 in the length of the incubation period, clinical severity, and transmissibility [8]. Despite government initiatives to implement social habits such as social distancing and wearing masks, and despite quarantining and non-pharmacological and preventive treatments for psychophysical wellbeing, the global spread of COVID-19 has increased [9, 10].

COVID-19 has unique imaging characteristics that constitute a visual identity when viewed through a radiologist's lens. Furthermore, COVID-19 adversely affects organs other than the lungs [11,12]. Due to these circumstances, research on this topic has exploded, with nearly **72,000** COVID-19-related articles published since December 2019 (see PubMed website [13]). This translates to an average of **2000 articles per week.** Interestingly, more than **900** articles are on COVID-19 and artificial intelligence (AI); these articles cover the models of machine learning (ML), transfer learning (TL), and deep learning (DL) (see Fig. 2 (d)). It appears that AI can play a role in the characterization of ARDS in the lungs and the characterization and diagnosis of other parts of the body [14]. The topic of AI for ARDS characterization must be investigated carefully to help practitioners better manage viral COVID-19 pneumonia leading to ARDS.

AI is involved in many facets of COVID-19 management, such as medical imaging, risk assessment, telemedicine, and patient follow-up [16]. Even though AI has penetrated into several fields of radiological imaging [17], such as classification of images into **(a)** controls, **(b)** community viral pneumonia, and **(c)** COVID-19 pneumonia [18–20], the question that remains unanswered is whether these models actually function the way the pulmonologists and critical care physicians want. For example, if the patient has a specific pre-existing disease, can an AI include this information into its knowledgebase and use it to more effectively correlate this comorbid condition, the age factor, and the grayscale patterns in lung scans with COVID-19 severity? Furthermore, there are other questions worth addressing, such as the following: (**i**) What kind of imaging modalities are useful for ARDS? (**ii**) What kind of image-based classifiers are most beneficial for detecting and classifying ARDS severity while also considering comorbidity, age group, and imaging characteristics? (**iii**) How can COVID-19 severity due to ARDS be measured? (**iv**) How should we estimate the survival of patients affected by ARDS? (**v**) How does a pre-existing disease or comorbidity affect the mortality from ARDS? (**vi**) What methods (new/hybrid) can be used to detect and classify the early stages of ARDS? All these issues must be addressed if valid diagnoses are to be given and if the therapeutic

---

[1] Quotation from Wikipedia [https://en.wikipedia.org/wiki/Syndemic]: "A syndemic or synergistic epidemic is the aggregation of two or more concurrent or sequential epidemics or disease clusters in a population with biological interactions, which exacerbate the prognosis and burden of disease."

applications of the AI framework are to be evaluated accurately.

The most popular medical imaging tools used for lung imaging are ultrasound, X-rays, CT (see Fig. 2: (a) Hyper-echoic region of the COVID-19 lung, 2 (b) The infected region in the lung, and 2 (c) Segmented lung region), and a recently developed technique that combines PET and CT to visualize the lungs and their metabolic functions [21–23]. This study considers various schools of thought for AI-based solutions for COVID-19 lung severity classification. Specifically, this study considers machine learning (ML), transfer learning (TL), and deep learning (DL) techniques, and combination of these. It also discusses the crucial issues and concerns that ongoing AI-based COVID-19 research must tackle to help the medical community.

This review makes the following contributions. (**i**) It is the first review of its kind that explores the pathophysiological aspect of acute respiratory distress syndrome (ARDS) due to COVID-19. It explicitly discusses the deteriorating alveolar stages leading to the gas-exchange disorder. (**ii**) This study is the only one that links the derived comorbid conditions and ARDS from nearly fifty studies. These conditions include hypertension, diabetes, obesity, chronic kidney disease, cardiovascular diseases, liver disease, hyperlipidemia, renal dysfunction, cancer, human immunodeficiency virus (HIV), lung disease, and cerebrovascular disease. Furthermore, it computes the link between comorbidity, ARDS, and mortality. (**iii**) The review compares the AI techniques used to characterize lung diseases during non-ARDS times (pre-COVID-19) with those used in ARDS times (post-COVID-19). (**iv**) This is the first review of its kind that develops the seven different school of thought (SoT) types utilizing AI techniques to evaluate the COVID-19 severity in the ARDS framework. (**v**) This is the only review that exclusively compares different imaging modalities for evaluating the lung conditions in ARDS. (**vi**) This is the first review of its kind that shows the evolution of AI design for personalized medicine by linking AI with ARDS having comorbidity. This is very useful for evaluating ARDS conditions in the COVID-19 framework.

The layout of the study is as follows. The research strategy is presented in section 2. The pathophysiology of ARDS is described in section 3. The effect of comorbidity with COVID-19 is analyzed in section 4. In section 5, AI architectures are divided into schools of thought (SoT). The practical aspect of AI for COVID-19 is explained in section 6. The critical discussion and conclusion are given in sections 7 and 8, respectively.

2. Research strategy

Fig. 3 shows the flowchart of our research strategy. We used four online research databases: PubMed, IEEE Xplore, ArXiv, and Web of Science. Initial screening used the keywords "COVID-19," "coronavirus," or "ARDS," with the modality terms "lung CT," "X-ray," or "ultrasound." The search was augmented with terms "artificial intelligence," "machine learning," or "transfer learning," or "deep learning," resulting in **1557** articles. We excluded **115** duplicate articles and articles that did not deal with COVID-19 severity (including classification), resulting in **1442** articles. Finally, we selected the articles based on our subjective assessment of their relevance and novelty, resulting in **399** articles. Excluding irrelevant articles, such as those that did not discuss comorbidity, resulted in **242** articles. Records with insufficient data were removed, leading to **230** resources. This was then used in our narrative study, which used AI-based, comorbid-based, and pathophysiology-based articles.

3. The pathophysiology of acute respiratory distress syndrome

The prime route of SARS-CoV-2 virus communicability is through the nasal droplets and saliva of an infected person [19]. The SARS-CoV-2 virus enters the alveolar type 2 cells (AT2 cells) by anchoring its viral spike proteins (S1 and S2) to the angiotensin-converting enzyme 2 (ACE2) receptor [24] (Fig. 4). Mossel et al. have reported that the previous coronavirus (CoV or SARS-CoV-1) replicates more aggressively in AT2 cells than in alveolar type 1 cells (AT1 cells) in the lung [25]. There is an 80% genetic resemblance between SARS-CoV-1 and SARS-CoV-2. It has been shown via molecular pathways [26] that SARS-CoV-2 has a high potential for binding with AT2 cells in the lungs [27].

In the inflammatory phase (marked as 3), inflammatory mediators are secreted as a systemic inflammatory response to the infection of AT2 cells by SARS-CoV-2 on the alveolar epithelium surface [28]. The secreted inflammatory mediators stimulate alveolar macrophage,
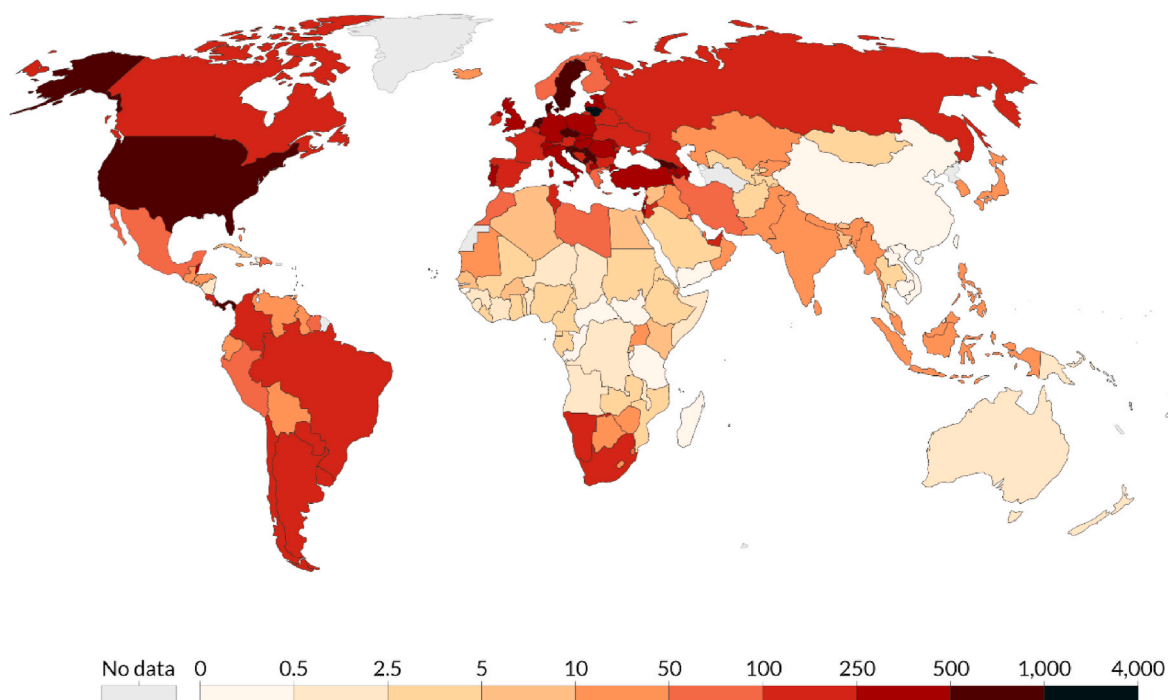

Fig. 1. Total confirmed cases per million as of December 21, 2020 [15]. (Source: Center for Systems Science and Engineering (CSSE) at Johns Hopkins University, Maryland, USA.).

producing cytokines like IL-1, IL-6, and TNF-α. In turn, the elevated production of cytokines and chemokines results in a condition called a cytokine storm. The sequence of the systemic inflammatory response, the cytokine storm, and the failure of multiple organs significantly influences ARDS's pathophysiology. These sequences can also be seen in all other viruses belonging to all CoV families (e.g., SARS-CoV-1 and MERS-CoV) [29,30]. This leads to the upregulation of trypsin.

Furthermore, it damages the endothelial tight junction protein and the zonula occludens, disorganizing and weakening endothelial cells and increasing these cells' vascular permeability to intravascular fluids [31]. In the dilatation phase (marked as 4), the cytokine storm causes endothelial barrier dysfunction. This is caused by the release of the cytokines following a viral infection. In the edematous phase (marked as 5), intravascular permeability leads to the diffusion of intravascular fluid (proteins, neutrophils, erythrocytes, and platelets) to the sub-alveolar and interstitial space, thereby causing diffused alveolar and interstitial exudates, as well as alveolar edema. At this point, one can observe radiological consolidations using lung CT as a diagnostic approach, and monitor the treatment prognosis [32]. Diffused alveolar and interstitial exudates and increased sub-alveolar edema are the hallmark features of ARDS [33].

During the alveolar collapsing phase (marked as 6), increased tension (due to the drowning of alveoli in the fluid accumulated in the sub-alveolar and interstitial space) causes alveolar collapse, which results in the disruption of gas exchange from alveoli [34]. The alveolar gas-exchange disorder (marked as 7) occurs because of the ventilation-to-perfusion mismatch between carbon dioxide and oxygen. This condition leads to hypoxemia and ARDS (marked as 8). This leads to increased mortality if left untreated [35].

4. Comorbidity and ARDS

Comorbidities of COVID-19 in ARDS include (i) old age, (ii) ethnicity, (iii) hypertension, (iv) diabetes mellitus (DM), (v) elevated BMI, (vi) cardiac diseases, and (vii) respiratory disorders. Studies have shown that ARDS tends to be worse among older patients [36–38], African Americans (Blacks in general) [39], and those suffering from hypertension [36,40], diabetes [36,38,41], BMI [42–44], respiratory diseases [42], and myocarditis [45–47]. These comorbidities play a vital role in segregating AI models that can be independently trained for effective diagnosis and COVID-19 severity prediction. The selected comorbidity studies [48–101] were taken from https://pubmed.ncbi.nlm.nih.gov/. Fig. 5 shows the number of subjects with comorbidities enrolled in the ARDS-based studies.

We used the following criteria during the selection process. The chosen keywords were hypertension, diabetes, obesity, chronic kidney disease, cardiovascular diseases, liver disease, hyperlipidemia, renal dysfunction, cancer, human immunodeficiency virus (HIV), lung disease, and cerebrovascular disease. The percentage of comorbidity subjects is shown in the pie chart as depicted in Fig. 6. This was designed
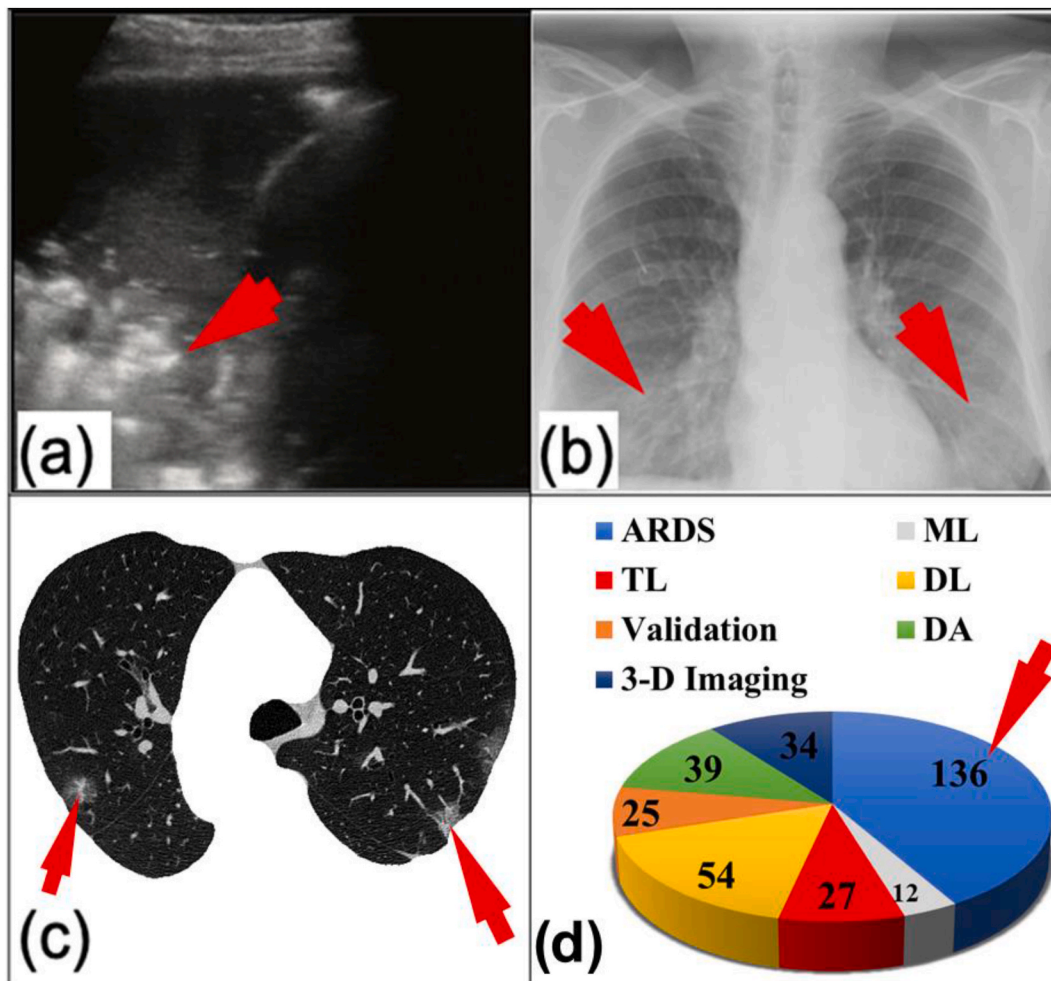

Fig. 2. Images of COVID-19 infection: **(a)** lung ultrasound (hyper-echoic region of the COVID-19 lung), (b) chest X-rays (the infected region in the lung), and **(c)** lung CT (segmented lung region; courtesy of Luca Saba, University of Cagliari, Italy). (d) The number of COVID-19 studies involving ARDS, ML, TL, DL, validation, data acquisition (DA), and 3-D imaging.
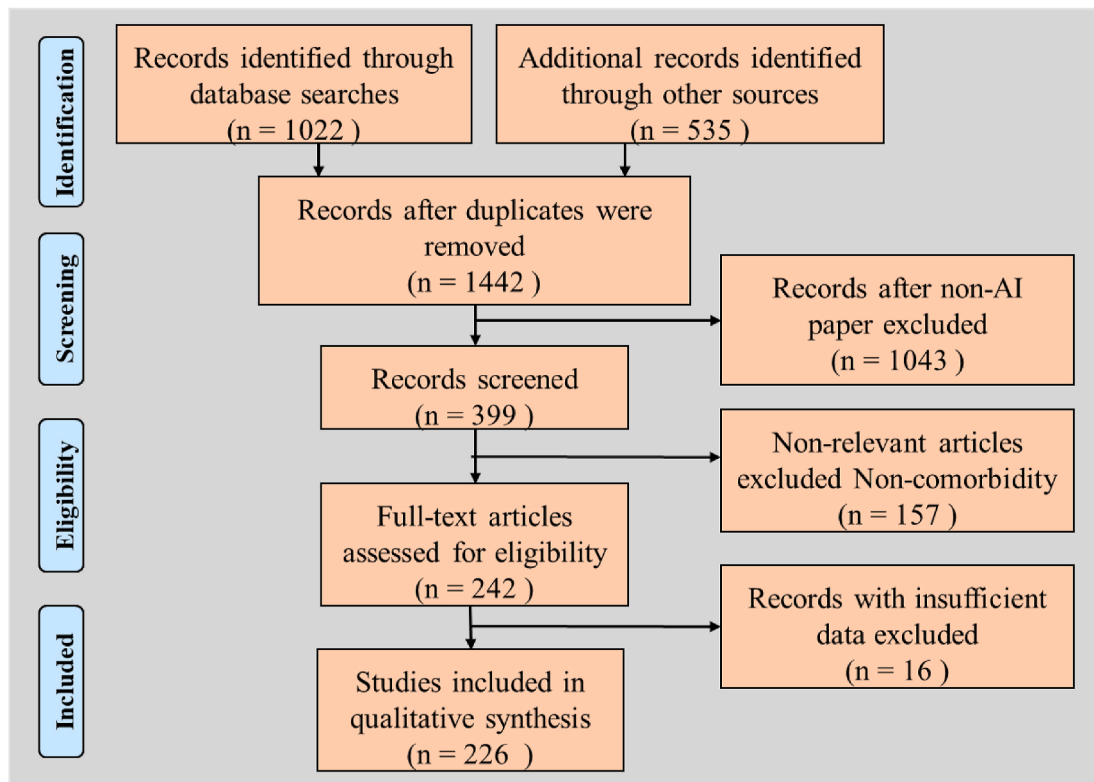
Fig. 3. The flowchart showing the research strategy.

using the selected 48 studies. Note that these 48 studies were pure medical journals discussing the role of comorbidity ("pre-existing diseases") and "age groups". Therefore, we decided to only consider these studies as a rationale and motivation for statistical data collection, which was likely to be helpful in the design of the innovative AI solutions for COVID-19 severity diagnosis and monitoring. The two most important contributing factors to COVID-19 were diabetes and hypertension, which together account for about **68%**. The rest of the comorbid predictors were nearly the same, in the range of **4%–13%**. The selected studies stated that a total of **14%** deaths were due to comorbidities in the ARDS framework. This pie chart demonstrates that comorbidity plays a vital role in the mortality of each cohort. Fig. 7 shows the distribution of the death due to the age factor with at least one comorbidity in the cohort. The most affected age range is **66–69,** with a total coverage of **58%** of the total cohort, followed by **age >70** with total of **20%** from the selected studies.

All these subjects had COVID-19 with one or more of these comorbidities. These comorbidities all contributed to the worsening of COVID-19. Thus, each comorbidity represents a category of the cohort whose imaging characteristics (or grayscale features) are likely to be similar. Therefore, multiple knowledge-based AI systems can be developed for each comorbidity using independent training cohorts. Based on these independently trained systems corresponding to each comorbidity, lung scans be characterized and COVID-19 severity can be assessed.

5. Artificial Intelligence architectures for ARDS characterization by school of thought

Characterization Definition. The concept of the characterization of the diseases using AI has been adopted in nearly all medical imaging areas. This includes the AI's role in pinpointing the disease, extracting the ROI of the disease, and automatically classifying the disease against binary or multiclass events. We have chosen machine learning and deep learning characterization systems that overlap and synchronize with

ARDS frameworks. The idea of using this characterization system is to share the origination and innovation spirits derived for different modalities and for different organs or applications. Note that some of these are taken from our own group intentionally to show the role of tissue characterization using AI or disease characterization using AI models. These systems are the crux solutions for diversification, which are unique and not available elsewhere. We specifically listed these as a "disease-specific portfolio" as a "one-stop-shop" to focus the search for the young scientists who are particularly interested in knowing how ARDS paradigms are related to other organ paradigms. Lastly, the third advantage of this cluster is to directly approach our group should more intricate details are necessary for such parallel characterization systems. Examples of AI-based characterization can be seen in several other body and disease applications, such as brain [102–104], stroke [105–107], plaque vascular wall [108–110], arrhythmia [111], liver [112–114], coronary artery [115,116], prostate [117], ovarian [118,119], diabetes [120], thyroid cancer [121], skin cancer [122,123], heart [124–126], gene expression [127], and rheumatoid arthritis [128]. This characterization framework can be extended to the ARDS framework.

Non-ARDS vs. ARDS. ARDS studies have started after December 2019. On the other hand, lung segmentation and classification techniques under the non-ARDS framework have existed for several years before the start of SARS-CoV-2. Some of the AI models used for non-ARDS lung data have been partially tried on ARDS lung data. For this reason, we have listed non-ARDS AI models against the ARDS AI models under three categories: segmentation, classification, and sub-regional applications (nodule, cancer, and tumor segmentation). This paper does not cover non-ARDS AI models or techniques. Table 1 shows the studies done in both non-ARDS and ARDS frameworks. The non-ARDS AI techniques were also applied to nodule, cancer, and tumor segmentation [129–136]. Note that we excluded (a) lung cellular images and (b) animal studies by considering only human lungs. Further state-of-the-art 2017–2020 studies were only considered for non-ARDS models, and validation and inter- and intra-observer variability studies were also not
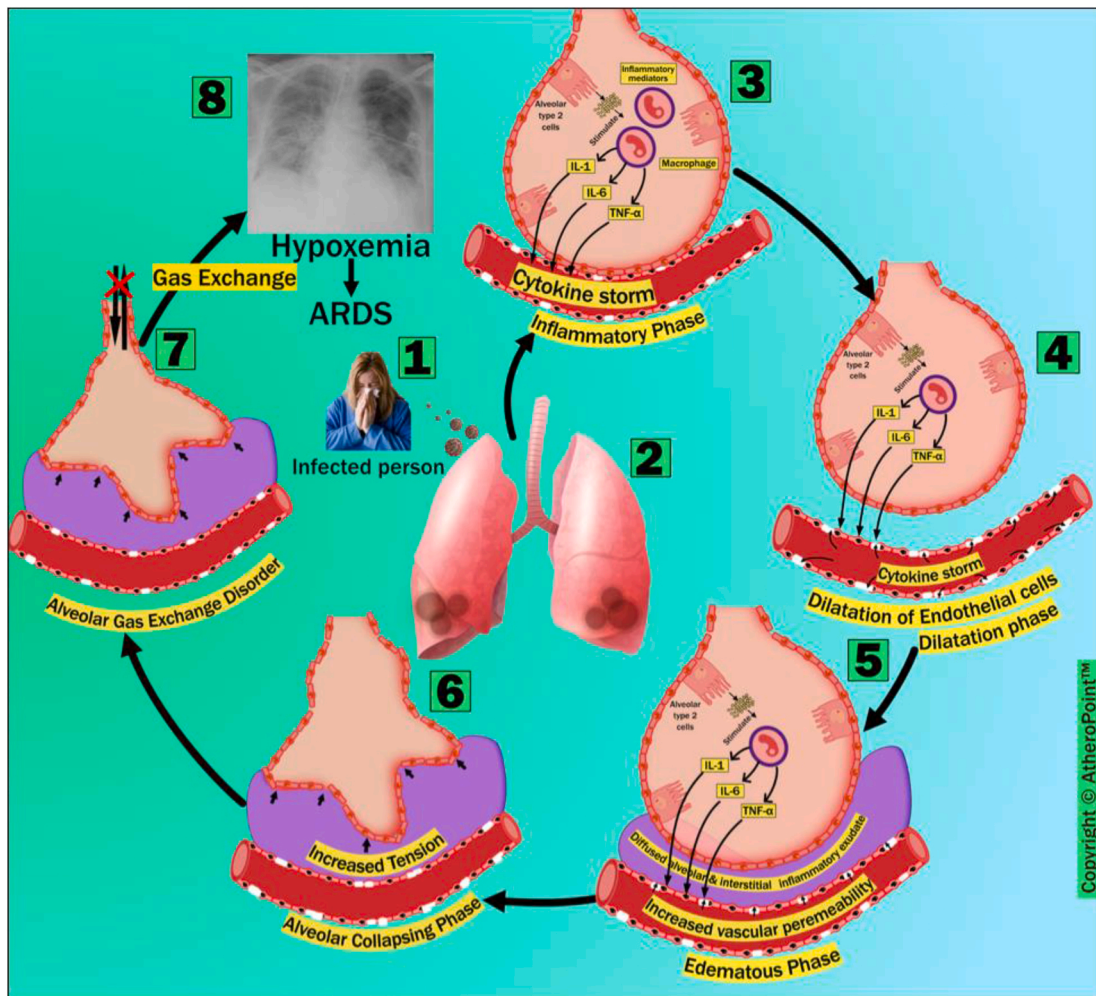
Fig. 4. The pathophysiology of ARDS after COVID-19 infection, which consists of six phases: **(i)** inflammatory phase, **(ii)** dilatation phase, **(iii)** edematous phase, **(iv)** alveolar collapsing phase, **(v)** gas-exchange disorder, and **(vi)** hypoxemia. (Courtesy of AtheroPoint™, Roseville, CA, USA; reproduced with permission.)
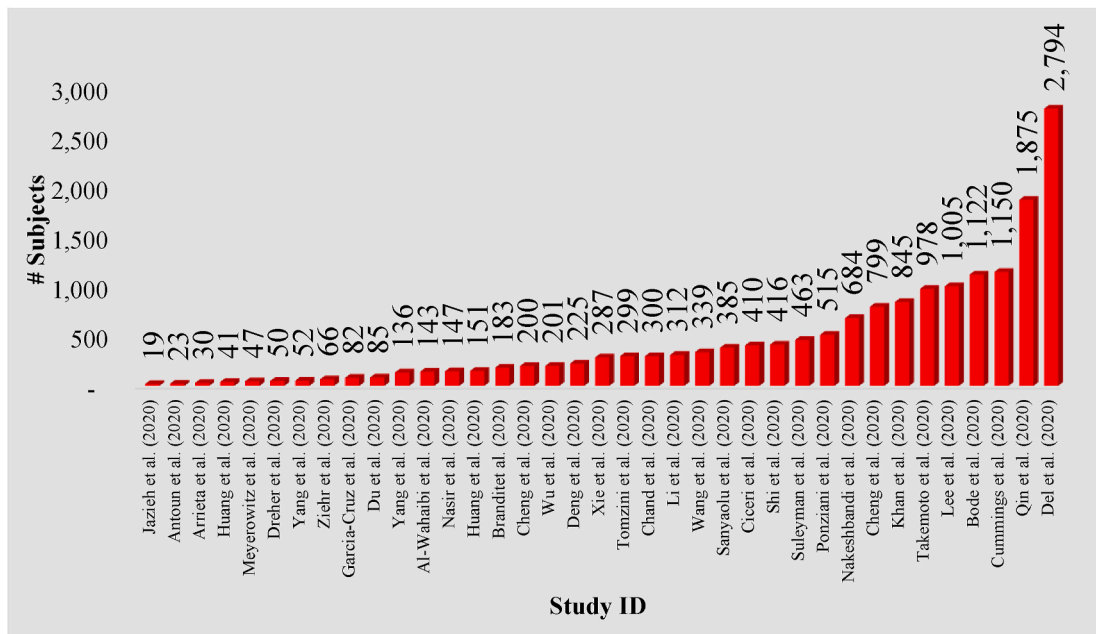

Fig. 5. The number of subjects enrolled in the ARDS-based studies that consider comorbidities.
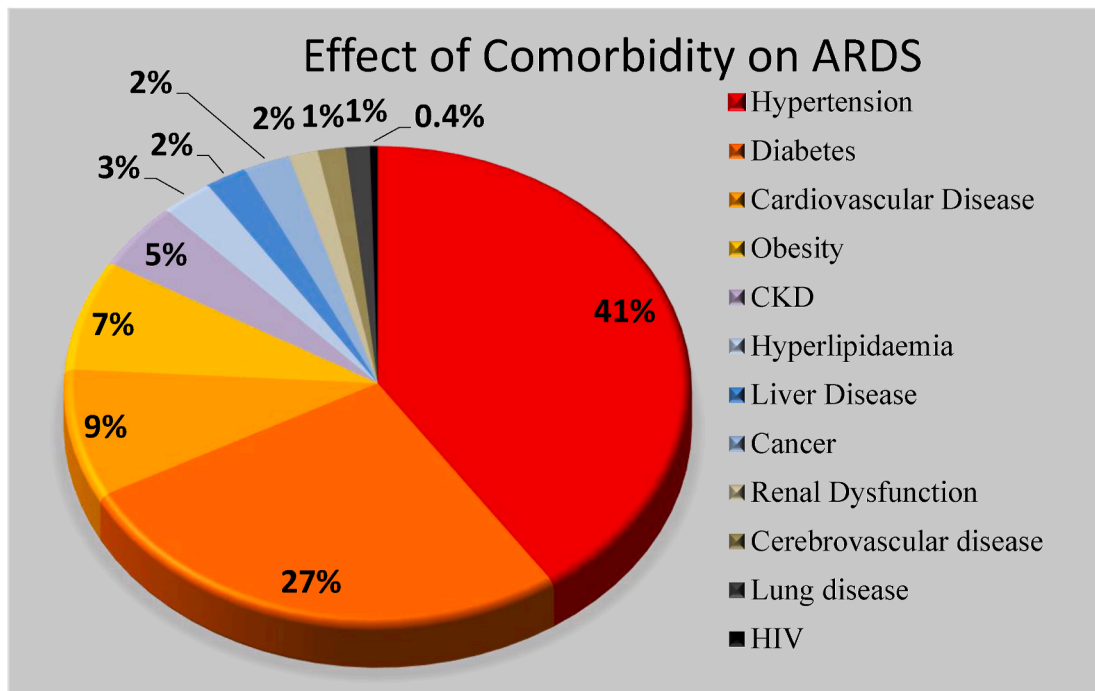
Fig. 6. Depiction of comorbidities collected from 48 studies.
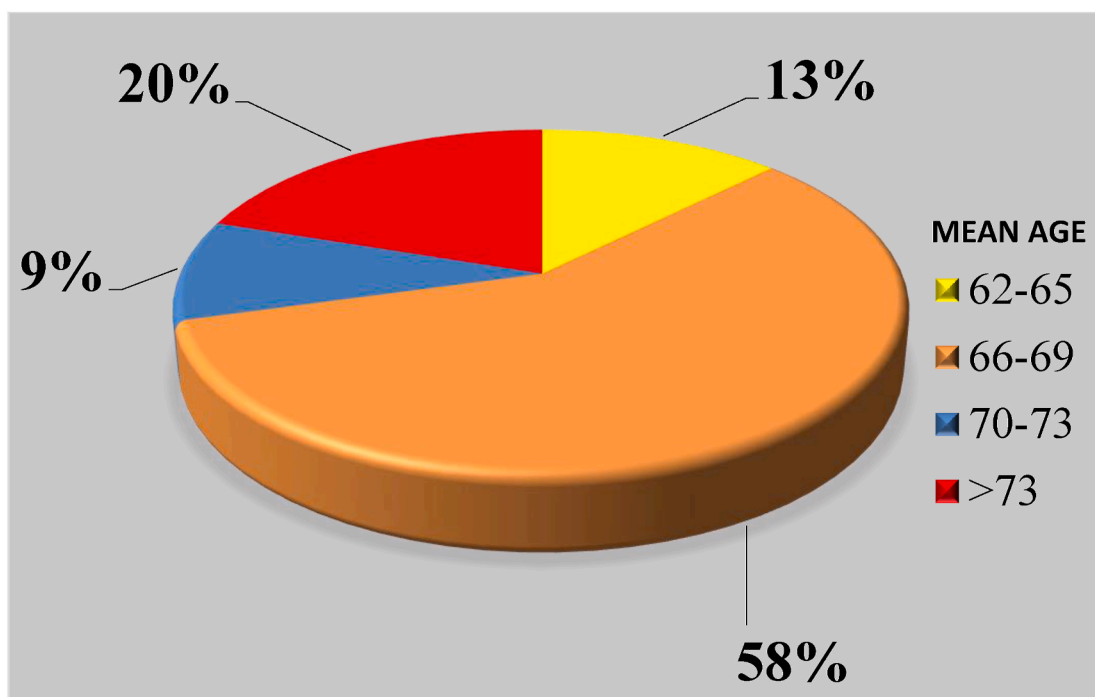
Fig. 7. Mortality due to the age factor (in years) with comorbidities in the cohort from the selected studies.

considered in Table 1.

It is essential to note that there are three typical components of an AI-based ARDS system: (a) segmentation of the lung region, (b) classification component, and (c) COVID-19 severity measurement (see Table 2). For the ARDS framework in this narrative review, we have proposed and classified the literature based on architecture (or so-called school of thought (SoT)) (see Table 3).

Definition of Schools of Thought and Their Relationship to AI Architectures. The classification of the AI architecture has been central to

different engineering applications. Imaging has been the most prominent AI application. Recently, Biswas et al. [17] presented a class of AI architectures for medical imaging. In our current study we present several applications using different classes of architectures (SoT). Biswas also discussed the evolution of architectures in terms of the present and future of deep learning [16].

These architectures can use the manual or automated feature selection method. Typically, manual feature selection methods were used in the past, where the features were hand-picked and fed to the

Table 1

AI-based studies involved during Non-ARDS and ARDS periods. AI-based Non-ARDS: AI on ARDS lung data during pre-COVID-19. AI-based ARDS: AI on ARDS lung data postmarked December 2019 COVID-19 (post-COVID-19).

Subsystems	AI-based Non-ARDS	AI-based ARDS
Segmentation	Characteristics Watershed, region-based, contour-based, fusion-based, and model-based. References [129,137–146]	Characteristics FC-Densenet103, Unet, DenseNet, and DenseNet121-FPN. References [147–165]
Classification	Characteristics Gray scale feature extraction and ML classifier, and model-based techniques. References [166–170]	Characteristics Resnet-50, CNN, SVM, ResNet101, VGG16, and VGG19. References [148,150–153,157–159, 171–175]
Joint Segmentation and Classification	Characteristics They use the same characteristics as adapted by segmentation and classification domain for AI-based Non-ARDS. References [167,169,170]	Characteristics They use the same characteristics as adapted by segmentation and classification domain for AI-based ARDS. References [148,150,151,154,156–159, 162]

Table 2

Types of artificial intelligence architectures and severity index.

SN	AI Components and Attributes		
	Lung Segmentation	AI Component	Severity Index
	Auto/Semi-Auto	ML/DL/TL/DL[a]ML/DL[a]TL	Categorical/Continuous/Categorical[a] Continuous
1	Auto	DL	Categorical[a] Continuous
2	Auto	DL[a]ML	Categorical[a] Continuous
3	Auto	DL	Categorical
4	Semi-Auto	DL[a]ML	Categorical[a] Continuous
5	Auto	ML	Categorical[a] Continuous
6	Auto	DL[a]TL	Categorical
7	Auto	TL	Categorical

[a] Both technologies are present.

classification model during its learning and training process. These were older generation methods. In other words, this is an old school of thought. Since the evolution of the concept of mimicking the brain using a greater number of layers for filtering the features, deep learning emerged. The main characteristic of deep learning (DL) paradigms is the ability to compute millions of training parameters automatically. This is a more recently evolved subset of ML. These methods are another, more recent school of thought. Thus, the schools of thought are primarily defined by their foundational architecture.

Although the AI industry is dominated by these two paradigms, it continues to look for alternatives. DL begins to look outdated, and more advanced architecture has started to emerge. For example, the challenges of DL during training have led to generating pre-trained weights to speed up and simplify the DL systems. This type of architecture is known as transfer learning. It is considered a more recent SoT and a classic in its category. In summary, the classification of the architectural has been synchronized more as a SoT based on the ingredients and components of the architecture. This is similar to the way segmentation of images many years ago was categorized into several architectures or SoT. For example, segmentation can be classified as region-based, contour-based, or knowledge-based. The categories were then fused together to generate intermediate architectures. These were known as fused architectures, and they combined region and contour or region with knowledge, generating another architectural paradigm or SoT. This

can be seen in the classic papers by Suri [176–178].

Therefore, a SoT is a synonym for architectural design, where the individual and fused architectures are each considered a SoT. Fused architectures have been developed by different groups around the globe and are presented in the literature. Thus, the SoT is a more refined version of an architectural design. In summary, the idea of the School-of-Thought it to make it more granular rather than being too binary. Some of our previous studies have used the school of thought concept. Please note the SoT are technically the same as the generations of architectures; however, they give more subtle differences.

The AI models used in different SoT along with their salient features are listed below.

SoT-1 is useful for obtaining a quantitative measurement of the extent of COVID-19 lung damage and classifying the lung within the binary and multiclass frameworks. Lung segmentation is automated without human intervention, using either commercial software, such as XMedCon [179], or AI techniques, such as threshold segmentation [180] or UNet-based segmentation [146]. The AI component is state-of-the-art or custom deep learning (DL) architecture.

The purpose of **SoT-2** is similar to that of **SoT-1** (to quantitatively and categorically estimate COVID-19 severity). However, researchers have employed a hybrid architecture that is more complex than the architecture of **SoT-1**.

Nevertheless, by blending multiple AI architectures (DL and ML), **SoT-2** has generally achieved comparable accuracy and accomplished additional sub-goals (e.g., prognosis analysis). The disadvantage of **SoT-2** is the time and effort required for the amalgamation and fine-tuning of discrete AI components.

SoT-3 is used only to divide patients into two or more classes (e.g., COVID-19, non-COVID-19, and other kinds of pneumonia). The majority of the AI-based COVID-19 research follows **SoT-3**. Lung segmentation before classification is automated, just like in SoT-1. SoT-3 involves an end-to-end automated pipeline with the primary goal being classification in one of several categories of pneumonia, including COVID-19. Because of this, it is faster (and often easier) to carry out research using SoT-3. The primary disadvantage of SoT-3 is that it offers few insights that healthcare professionals can apply to treat COVID-19-infected patients. For example, SoT-3 does not help quantify biomarkers that represent the severity of the disease.

SoT-4 involves the semi-automatic segmentation of lungs from radiography images by professionals before use for AI-related processing. Multiple metrics are computed using an AI component that is a hybrid of various AI architectures. SoT-4 gives researchers the freedom to create a pipeline with the appropriate balance of accuracy, speed, and complexity, depending on the desired metrics. The disadvantage of SoT-4 is that designing the semi-automatic segmentation of lungs and the appropriate hybrid models takes a fairly long time.

In **SoT-5**, researchers use automated lung segmentation, but they also use traditional machine learning (ML) models, hand-crafted feature engineering, and feature selection methods. The computed features are then used to compute biomarkers, which, in turn, are used to predict the severity of COVID-19 and to classify patients. Research belonging to **SoT-6** uses automated segmentation with a hybrid model of DL and TL to produce a categorical metric for classifying patients. Finally, **SoT-7** research is similar to **SoT-6**, with the sole difference being that the transfer learning (TL) model is the primary component [181]. It contains two components: an offline system and an online system. Relevant features are extracted manually by the researchers using radiography images. These features are then passed on to a classifier in an offline system for training. Once the offline system is trained, the training coefficients are transferred to the online classifier, which is then used for real-time classification and severity prediction. ML can also be effectively used to segment the lungs in medical images, as shown in Refs. [146,167]. An online ML-based COVID-19 risk prediction system is depicted in Fig. 8. This is very much along the lines of previous ML systems published by our group [165,182,183].

Table 3

Clustering of multimodality artificial intelligence architectures and their salient features.

| SoT	Reference	Modality	Imaging	Highlight/Objective	Architecture Description	Performance Metrics
SoT-1	[147–153, 229]	**CT** [229]: [147, 148] **X-ray** [149]: [151] **LUS** [150]:	**3-D** [229]: [147,148] **2-D** [149]: [150, 151]	Multiview fusion [229], Multi-view pyramid network with attention [147], training using human in loop [148], video-based real time prediction [150], end-to-end DL architecture for semi quantitative prediction COVID- 19 severity [151]	Resnet50 [229], Custom CNN with attention [147], VB-Net [148], commercial deep learning system by Lunit Inc [149], Spatial Transformer Net- work [150], ensemble of multiple networks (Backbone – ResNet, VGG, DenseNet, Inception; Segmentation- UNet, UNet++; Alignment- Spatial Transformer Network; Scoring Head-Feature Pyramid Network; Custom Network) [151]	**ACC** [229]: [147,148,150, 151] **AUC** [229]: [147] **Sensitivity** [229]: [149, 150] **Specificity** [229]: [149] **Others** [148]: [149–151]
SoT-2	[152,153]	**CT** [152]: [153] **X-ray: LUS:**	**3-D** [153]: **2-D** [152]:	Biomarker based model [152], model for severity in 3-D lung abnormalities [153]	Resnet34 with logistic regression [152], Dense UNet [153]	**AUC** [152]: **Others** [152]: [153]
SoT-3	[154–156, 171,173, 174]	**CT** [154] [155,171] [156,173] **X-ray:** [157,174] **LUS: NA**	**3-D** [154]: [173] **2-D** [171]: [155–157,174]	3-D Convolution Network [154], multi-objective differential evolution based CNN [171], comparison of ten CNNs [156], weakly supervised DL model [173], truncated InceptionNet [174], modified DarkNet CNN [157]	Resnet50 [154], Custom CNN [157,171,173], DenseNet [155] (AlexNet, VGG-16 VGG-19, SqueezeNet, GoogleNet, MobileNet-V2, ResNet-18, ResNet-50, ResNet-101, and Xception) [156], InceptionNetV3 [174]	**ACC** [171]: [155,156,173, 174] [157] **AUC** [154]: [155,156,173, 174] **Sensitivity:** [154,155,171] [156,157,173, 174] **Specificity** [154]: [155, 171] [156,157,173, 174] **Others** [171]: [155–157,173, 174]
SoT-4	[157]	**CT** [157]: **X-ray: NA LUS: NA**	**3-D** [157]: **2-D**: NA	ML and DL hybrid network for classification and prognosis [157]	Resnet18 with Gradient Boosting [157]	**ACC** [157]: **AUC** [157]:
SoT-5	[158,159]	**CT** [158]: **X-ray: NA LUS** [158]:	**3-D:NA** **2-D** [158]: [159]	Pleural line identification using ML [158], automatic severity assessment and exploration of severity related features using ML [159]	Hidden Markov Model and Viterbi Algorithm combined with SVM [158], Random forest [159]	**ACC** [158]: [159] **AUC:** [[159] **Sensitivity** [158]: **Specificity** [158]: **Others** [158]: [159]
SoT-6	[160,172]	**CT** **X-ray** [160]: [172] **LUS:**	**3-D:NA** **2-D** [160]: [172]	Ensemble of DL and TL [160], multi-dilation CNN for extraction of COVID-19 features [172]	Custom CNN [160,172], (VGG- 16, VGG-19, Inception-V3, Xception, InceptionResNet- V2, MobileNet- V2, DenseNet-201, NasNet- mobile) [160]	**ACC** [160]: [172] **AUC** [160]: [172] **Sensitivity** [160]: [172] **Specificity** [160]: [172] **Others** [160]: [172]
SoT-7	[161–165, 175]	**CT** [165]: **X-ray:** [163–165,175] **LUS** [161]:	**3-D:NA** **2-D** [175]: [161–165]	Explainable DL to provide explainability about the prediction [175], real time internet based COVID-19 detection service [161], TL model trained on ensemble of two publicly available datasets [163], interpretable AI framework for COVID-19 classification [164], applying TL on comprehensive custom COVID- 19 CT and X-ray datasets [165]	VGG-16 [161,175], Alexnet [165] DenseNet201 [162], Xception [163], InceptionNetV3 [164]	**ACC** [175]: [161–165] **AUC** [161]: [162,164] **Sensitivity** [175]: [161–165] **Specificity** [175]: [161–165] **Others** [175]: [161–164]
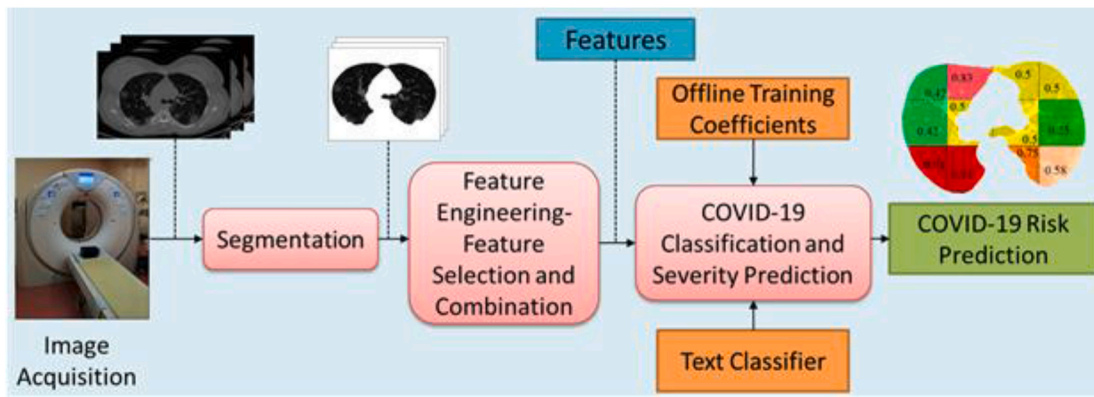
Fig. 8. An online ML-based COVID-19 risk prediction system. (Courtesy of AtheroPoint™, Roseville, CA, USA; reproduced with permission.)
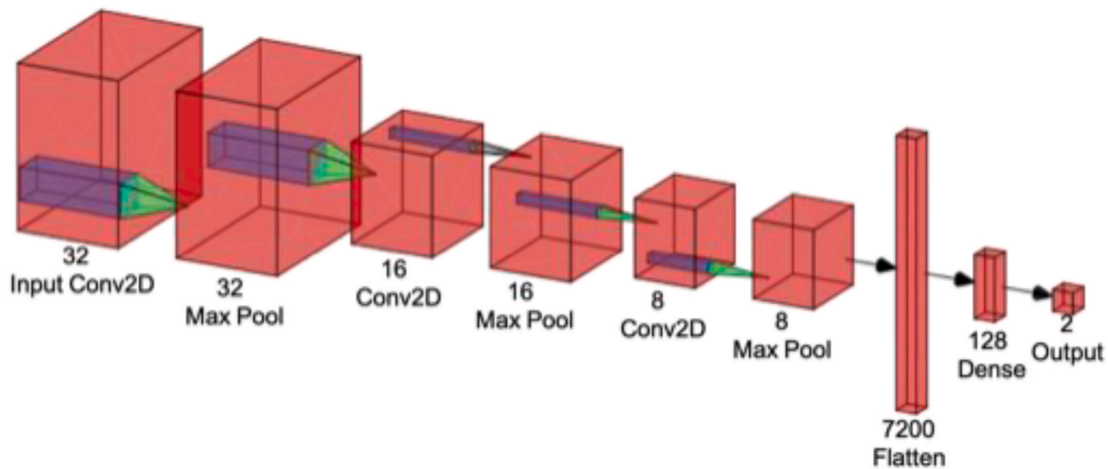

Fig. 9. A custom CNN-based DL architecture comprising different layers.

A reference DL architecture created using [184] is shown in Fig. 9. The most commonly used type of DL architecture is the convolution neural network (CNN). This network consists of multiple convolutional filters that extract simple visual features from the image data. Multiple CNN filters are stacked together in layers so that complex visual features can be extracted from the image data. The CNN layers are often bundled together with pooling layers to reduce the spatial information contained in the intermediate representation and padding layers, thus maintaining the appropriate dimensions of the data.

TL is an extension of state-of-the-art DL architectures that are pre-trained using massive datasets. TL techniques produce more accurate results when there is less training data, when the available hardware has fewer capabilities, or when little training time is available. The reference architecture of TL created using [185] (called VGG16) is shown in Fig. 10.

Table 3 presents a comparison of multi-modality AI architectures for COVID-19 diagnostics, along with their salient features. The "Arch Type" refers to the seven SoT architectures that we have devised after clustering various AI research works based on their workflow and intent. The "Reference" and "Modality" attributes are self-explanatory. The "3-
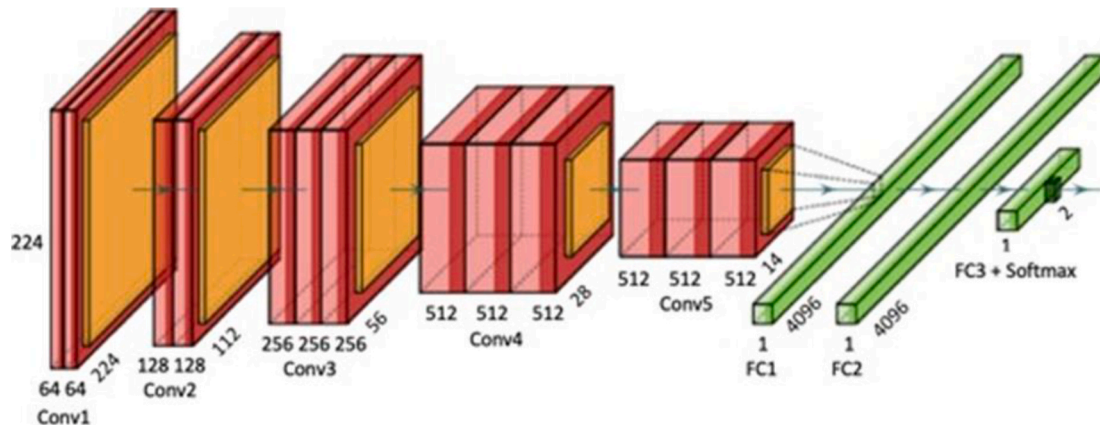

Fig. 10. An example of transfer learning (TL) architecture using VGG16.

D/2-D Imaging" attribute shows whether the research has used two-dimensional or three-dimensional radiological imaging [186,187].

The "Highlight/Objective" attribute represents the distinguishing feature of the research. The "Architecture Description" attribute describes the underlying base AI architecture adapted in the study. The "Performance Metrics" attribute shows which metrics the researchers had used to validate their work. Readers are encouraged to look into dedicated AI-based reviews for a deeper understanding of AI and its applications.

6. Workflow considerations for COVID-19 lung characterization: CT vs. X-ray

The three chest imaging modalities X-ray, CT, and ultrasound have been strongly recommended by WHO for the diagnosis of COVID-19 [90]. In their guidelines, the following observations were given for COVID-19 diagnosis. (i)) X-rays was found to be lower in sensitivity and higher specificity than chest CT imaging [188,189]. (ii) Chest X-rays are less expensive, have lower radiation, takes less acquisition time, and are less expensive to use for monitoring than CT. (iii) Chest CT was found to have higher sensitivity but lower specificity and emits more radiation than X-ray. (iv) Lung ultrasound was found to have very low diagnostic accuracy but offers an alternative for several other applications, such as the abdomen, carotid, urology, obstetrics, and gynecology imaging. On the other hand, ultrasound has a high risk of COVID-19 infection transmission due to close contact with the patient compared to other imaging modalities. Meanwhile, MRI is a popular imaging modality for diagnosing many severe diseases. However, according to the guidelines of the American College of Radiology (released on April 8, 2020) [190], MRI is not recommended for COVID-19 patients due to the high risk of infection [91]. The literature includes studies covering MRI and COVID-19 [92–94]; however, no relevant literature was found where MRI, COVID-19, and AI were all mentioned, mainly due to the high cost, long scanning time, and high risk of infection. FDG-PET/CT [191] imaging is another high-level imaging technique that was used in many studies to diagnose COVID-19 [95,96]. PET/CT is a more advanced imaging technique than CT alone; however, it is more expensive [23, 192]. We did not find any relevant studies for the diagnosis of COVID-19 with FDG-PET/CT imaging that used AI. The suitability of X-ray and CT imaging for COVID-19 (see Fig. 11), based on recommendations by WHO, is shown in Table 4, where we discuss the workflow and the practical implementation. The major studies for automated COVID-19 diagnosis using the AI paradigm with X-rays and CT are [21–23, 192–202]. Due to their popularity in the scientific community, there are several open-source COVID-19 datasets available for X-ray and CT imaging modalities, such as the one from RSNA (https://www.rsna.org). The percentages of studies using X-ray, CT, or both, shown in Fig. 11(c), are 58%, 37%, and 5%, respectively, with CT considered the gold standard. These studies were chosen because of the completeness of their AI models and the attributes governing them. The following

Table 4

Compatibility of imaging modality for COVID-19 and adaptability for AI [230].

Imaging Modality	Suitable for COVID-19 as per WHO guidelines	Cost	Risk of radiation	Risk of infection due to close contact	Compatible with AI for COVID-19 diagnosis
PET/CT	High	Very High	Very High	Low	Low
CT	High	High	Very High	Low	Very High
X-ray	Medium	Low	High	Low	Medium
Ultrasound	Low	Low	No	High	Low
MRI	Low	High	No	Low	Low

attributes were considered for comparing X-rays and CT: (i) number of subjects, (ii) risk classes, (iii) 2-D vs. 3-D imaging, (iv) automated vs. non-automated ROI segmentation, (v) AI models, (vi) augmented vs. non-augmented, (vii) K-fold cross-validation, (vii) hardware and software, (ix) optimal models, and (x) performances. Based on these attributes, the studies on X-ray and CT imaging modality for automated COVID-19 diagnosis are compared, respectively, in Tables 5 and 6. For the **1**st **attribute** (number of subjects), some remarkable studies were found ([203–208]) that used a cohort of over 1000 subjects. The **2**nd **attribute** (number of classes) was broadly divided into binary and multiclass. More than half of the selected studies had binary classification [203,204,209–216], while the rest had multiclass. For the **3**rd **attribute** (2-D vs. 3-D), two studies ([210,212]) used a 3-D CT volume as input, while the rest used 2-D X-ray images. For the **4**th **attribute**, ROI segmentation in chest images was an essential aspect prior to classification. Three types of ROI were observed; five studies ([203,211,212, 217,218]) used automated ROI segmentation criteria, and only one study ([209]) adopted manual segmentation. Most studies used full-sized images for the classification.

The **5**th **attribute** (type of AI models) includes two main categories, ML- and DL-based studies. In one study on chest X-rays, images were classified as normal, pneumonia, other diseases, or COVID-19 using a DL-based network, with an accuracy of 90.13% [219]. Some of the images and their corresponding color maps are shown in Fig. 12. In another study, COVID-19 abnormalities were detected in lung CT scans using a DL-based network, and a heatmap of corresponding severity levels was generated [220]. The resultant images are shown in Fig. 13.

For the **6**th **attribute** (image augmentation), data limitation is always a big challenge for medical studies. Therefore, most of the studies used TL with DL models in such scenarios, especially when data is limited (i.e., in the thousands). Due to limited data, augmentation was applied to increase the data synthetically [210–212,215,218]. For this method, the images are synthetically increased using operations like image transformation (rotation, translation, and scaling), blurring, color jiggling, etc. There have been studies that use a patch-based framework with a relatively small number of trainable parameters for COVID-19
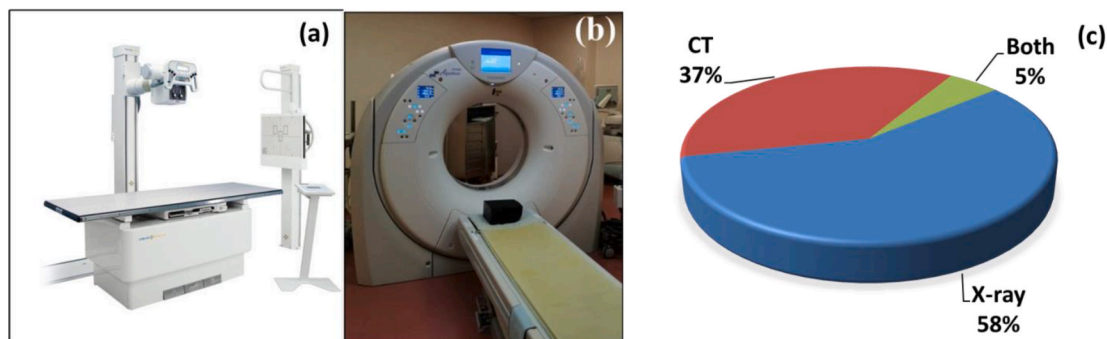

Fig. 11. (a) An X-ray scanner. (b) A CT-scanner (Courtesy of Luca Saba, University of Cagliari, Italy). (c) Studies using CT vs. X-ray.

Table 5
Artificial Intelligence-based studies for automatic COVID-19 detection using lung CT.

SN	Reference	[a]Subj.	Risk Class	2-D vs. 3-D	*ROI	AI Model	Augm.	CV	H/W-S/W	Optimal Model	Performances
1	Ardakani et al. (2020) [209]	194	2	2-D	×	CNN + TL	×	NA	SPSS software (version 24, IBM)	ResNet101	ACC:99.51% SE:100% SP:99.02% AUC:0.994
2	Wu et al. (2020) [217]	495	3	2-D	✓	CNN + TL	×	NA	GPU Python	ResNet50	ACC:76.0% SE:81.1% SP:61.5% AUC:0.819
3	Zheng et al. (2020) [210]	499	2	3-D	×	3-D CNN + TL	✓	NA	GPU PyTorch	UNet	ACC: 90.1% SE: 90.7% SP: 911% AUC: 0.976
4	Yang et al. (2020) [211]	679	2	2-D	✓	CNN	✓	NA	GPU PyTorch	DenseNet169	ACC:89% FS:90% AUC:0.98
5	Gozes et al. (2020) [212]	270	2	2-D & 3-D	✓	3-D + 2-D CNN	✓	NA	NA	Resnet50	SE: 98.2% SP: 92.2% AUC: 0.996
6	Shi et al. (2020) [203]	2685	2	2-D	✓	ML (RF)	×	K5	NA	RF	ACC:87.9% SE: 90.7% SP: 83.3% AUC: 0.942
7	Liu et al. (2020) [213]	746	2	2-D	×	LA-DNN + TL	×	NA	NA	LA-DNN	ACC:88.8% F1S: 94.7% AUC: 0.88
8	Panwar et al. (2020) [204]	2482	2	2-D	×	CNN + TL	×	NA	NA	VGG19	ACC:87.9% SE: 90.7% SP: 83.3% AUC: 0.942

[a] Subj.: Number of subjects in the study; Augm.: Augmentation; NA: Not available; ACC: Accuracy, SE: Sensitivity; SP: Specificity; AUC: Area under the curve; F-M: F-measure; KP: Kappa statistics; TL: Transfer Learning; FS: F1-Score LA-DNN: lesion-attention deep neural network; RF: Random forest; ML: machine learning; H/W: Hardware; S/W: Software; CV: Cross-Validation; K5: five-fold; ROI: Automated Region of Interest.

Table 6
Artificial Intelligence-based studies for automatic COVID-19 detection using lung X-ray.

SN	Reference	[a]Subj.	Risk Class	2-D vs. 3-D	Auto ROI	AI Model	Augm.	CV	H/W-S/W	Optimal Model	Performances
1	Narayan Das et al. (2020) [216]	NA	3	2-D	×	CNN + TL	×	NA	NA	Proposed CNN	ACC: 97% FM: 96% SE: 97% SP:97% KP:0.97
2	Ouchicha et al. (2020) [205]	2905	3	2-D	×	CNN	×	K5	NA	CVDNet (proposed CNN)	ACC: 90% PR: 96.72% RC: 96.84% FS: 96.68%
3	Hemdan et al. (2020) [214]	50	2	2-D	×	CNN	×	NA	GPU Python	VGG19 DenseNet201	ACC: 96.69% PR: 83% RC: 100% FS: 91%
4	Zhang et al. (2020) [215]	43,370	1, 2	2-D	×	CNN	✓	K5	NA	CAAD (proposed CNN)	ACC: 78.57% SE: 71.70% SP:79.40% AUC: 0.83
5	Togacar et al. (2020) [218]	458	3	2-D	✓	CNN + TL	✓	K5	CPU MATLAB	MobileNetV2	ACC: 99.24% SE: 100% SP: 97.72% FS: 99.43%
6	Farooq et al. (2020) [206]	2839	4	2-D	×	CNN + TL	✓	NA	NA	ResNet50	ACC: 96.23% RC: 100% PR: 100% FS: 100%
7	Cozzi et al. (2020) [207]	1427	3	2-D	×	CNN + TL	×	K10	NA	VGG19	ACC: 96.78% SE: 98.66% SP: 96.46%
8	Pereira et al. (2020) [208]	1144	7	2-D	×	ML + DL + TL	×	NA	NA	Multilayer Perceptron	FS: 89%

[a] Subj.: Number of subjects in the study; Augm: Augmentation; NA: Not available; ACC: Accuracy; SE: Sensitivity; SP: Specificity; AUC: Area under the curve; F-M: F-measure; KP: Kappa statistics; PR: precision; RC: recall; FS:F-Score; TL: Transfer Learning; LA-DNN: lesion-attention deep neural network; ML: machine learning; H/W: Hardware; S/W: Software; CAAD: confidence-aware anomaly detection model; ROI: Region of Interest.
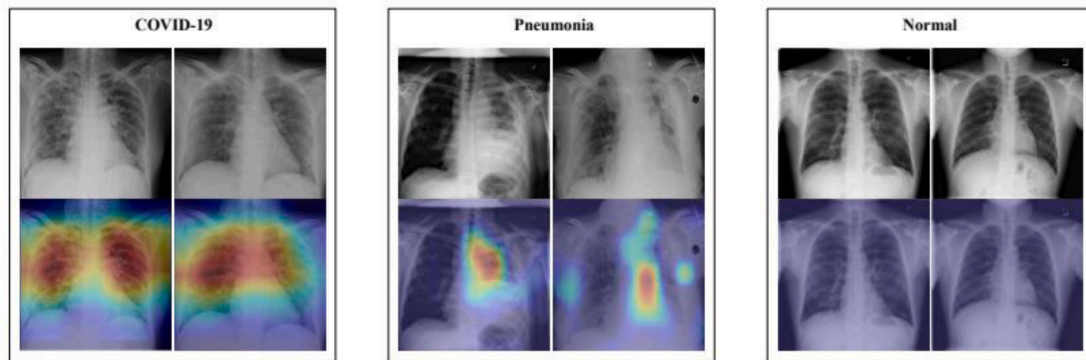
Fig. 12. X-ray scans of COVID-19, pneumonia, and normal lungs (Reproduced with permission [219]).
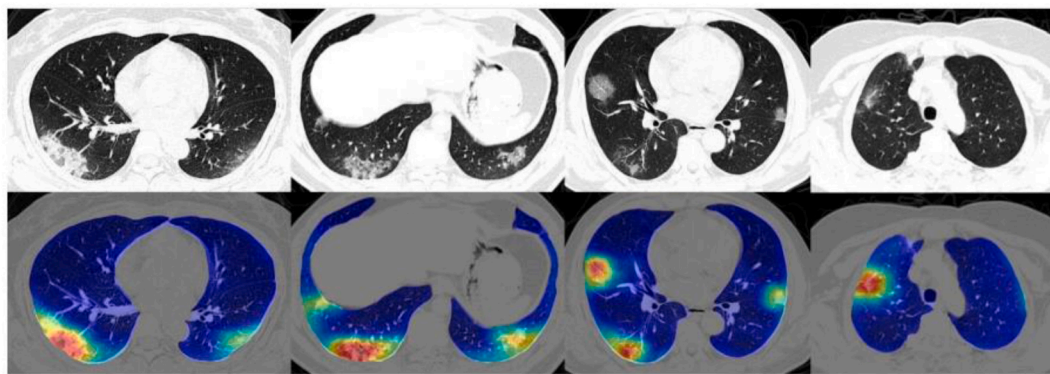

Fig. 13. CT scans classified as positive for coronavirus abnormalities and their corresponding color heatmaps (Reproduced with permission [220]).

diagnosis, and use multi-scaling for spatial features [221,222]. For the cross-validation (the **7**th **attribute**) of the data, the *K*-fold strategy was used to evaluate the performance of the AI technique. In this technique, *K* is the number of folds (or combinations) of training and testing samples.

In each round, the training is performed, and the model predicts the outcome based on the test sample. These predictions are compared against the gold standard to compute the ROI and performance of the AI system. Some authors ([203,205,215], and [218]) used five-fold CV, and one author [207] used ten-fold CV. The hardware constraints (the **8**th **attribute**) is discussed further in the critical discussion section. During optimization (the **9**th **attribute**) of the AI model, it is important to avoid overfitting. CV and TL were used to suppress over-fitting in supervised learning. Overfitting is a situation where the model can predict known data accurately, but is unable to predict unknown data. There are many ways to avoid overfitting; one of them is to use more data in the training model. The performance (the **10**th **attribute**) of the classifier depends on various factors, such as the number of subjects, the sample size, the training iterations, the training time, etc. Therefore, we cannot identify a single best-performing model or method at this stage. However, over time, as more studies and trials are conducted, the superior AI models will emerge.

7. Critical discussion

Clinical Requirements for COVID-19 AI Systems. An ideal AI system for COVID-19 must be robust and stable, and its output must vary within the acceptable limits with changes in the demographics or other patient-related characteristics. It must be reliable and reproducible; i.e., it must yield similar results across multiple trials. Furthermore, when used in an operating room, it must be reasonably fast and cost-effective compared to traditional COVID-19 diagnostic techniques (e.g., real-

time polymerase chain reaction (RT-PCR) tests). The AI system must be generalized by being trained and tested on an equal percentage of data. COVID-19 severity is a critical metric for doctors treating COVID-19 patients, and it is a desirable requirement of any AI diagnostic system.

Radiologists, pulmonologists, and doctors must validate the results of the AI system before its effectiveness can be determined. Finally, the AI system should segment the impact of COVID-19 on different organs using 3-D imaging to further assist clinicians. There is a vast potential for improvement for existing SoT using the AI-assisted diagnostics of COVID-19 patients by incorporating the above clinical requirements.

System Optimization. The majority of AI-based systems for COVID-19 detection and classification are based on DL. Several researchers have used data augmentation to increase the volume of COVID-19 data for training. The number of convolution layers is a hyperparameter that researchers need to adjust based on their intuition. However, DL-focused AI systems for COVID-19 need to be optimized based on the relationship between augmentation, the number of convolution layers, and classification accuracy (Fig. 14).

Scientific Validation. The behavior of an AI-based COVID-19 diagnostics system should be observed and validated under various comorbidity conditions. There are numerous scenarios in which the underlying assumptions may change. For example, the CT scan's thickness can be altered, or a different view of a CT scan (coronal, sagittal, and axial) can be given to the system for diagnostic purposes. Furthermore, the stability of a system must be validated by changing the combination of data that is used (e.g., K10, K5, K2, the so-called partition protocol). A stable AI system will yield a minimum standard deviation value across different data combinations [165]. The system should also be validated for patients from different age groups and with different comorbidities.

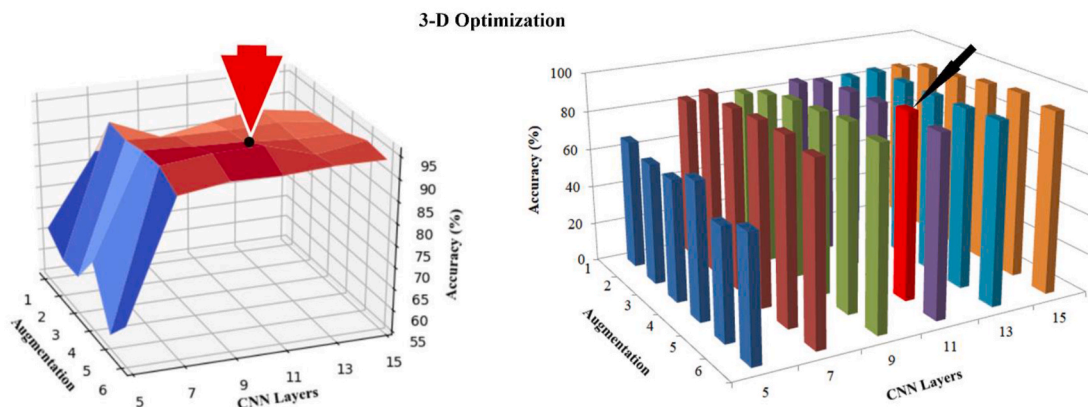*Clinical Validation.* In order for the research to be accepted by the

Fig. 14. A 3-D graph representing the relationship between CNN layers, data augmentation, and accuracy. (Courtesy of AtheroPoint™, Roseville, CA, USA; reproduced with permission [14].)

regulatory authorities, a gold standard validation should be performed through a physical examination of the body organs against the results predicted by the AI system. One way of doing this is through the microscopic validation of the body tissues for the severity of ARDS from COVID-19, as shown in Fig. 15. Inter-observer and intra-observer variability analysis [223] should also be performed to minimize any human bias in the system.

AI for COVID-19 Comorbidity and Age-Group Frameworks. The AI system must be designed to accommodate the patients' comorbidities (e. g., diabetes, cardiovascular diseases, obesity, retinopathy, pancreatic diseases, blood vessel diseases, and angiography [224]), along with their age groups. In Ref. [225], an AI system was developed to predict cardiovascular diseases in a multi-ethnic patient scenario. The AI systems designed in Refs. [226,227] can be extended to COVID-19 diagnosis by including comorbidities and age groups.

The primary AI system can be broken down into multiple subsystems for various comorbidity classes, with each comorbidity class having further subclasses for different age groups. For instance, if there are five comorbidities and three age groups, there will be 15 subsystems. Each subsystem should be trained separately using a different gold standard database [228]. The appropriate AI subsystem for a new patient can be determined by feeding additional input information about the patient's comorbidities and age group into the system.

3-D Image Acquisition and Processing. Most AI research for COVID-19 shows the severity of the lung infection in 2-D, which is undesirable because the disease progression cannot be depicted accurately in 2-D. It is therefore helpful to evaluate the COVID-19 data in 3-D (see Fig. 16). Scans of the Patients can be acquired during the contrast enhancement of a lung ultrasound [231]. A contrast agent, if included in the

bloodstream, aids the early management and prognosis of COVID-19. In Ref. [232], the authors used 3-D CT for diagnosis and classification of lung lesions affected by COVID-19. Recently, the authors in Ref. [233] used DensNet121-FPN for segmentation of the lung and classification using deep learning strategy.

Multi-Modality Data. Radiography provides many solutions for diagnosing COVID-19, like lung CT, chest X-rays, lung ultrasound, and PET/CT scans. The choice of modality depends on the patient's comorbidities, age, and pre-test probabilities (PTPs) [18]. A PTP test on troponin levels (which is an indirect indicator of hypoxia) can be conducted to identify the severity of a COVID-19 infection. During the initial phase of the COVID-19 infection, X-rays and lung ultrasounds can be useful owing to their low cost and easy obtainability, and to the small footprint of the medical device. However, if a patient has comorbidities, is elderly, or has COVID-19-induced ARDS (which leads to hypoxia), lung CT is likely the best modality due to its higher resolution and robust diagnostic capabilities. Any AI system for COVID-19 must be adaptable and generalizable to multiple modalities according to each patient's requirements.

Tissue Characterization of Lung Scans. In our previous work [3], we performed a bispectrum (B) analysis on COVID-19 lung tissues based on a higher order spectrum (HoS) to validate the survey results without using AI. The results (Fig. 17) confirm that COVID-19-infected samples possess much higher B-values than non-infected samples. Thus, AI can effectively exploit the underlying patterns to distinguish COVID-19 samples from non-COVID-19 samples.

Data Collection. It is desirable to collect data during a sizeable temporal window and from geographically distant locations, because this reduces biases related to age, comorbidity, ethnicity, and other factors
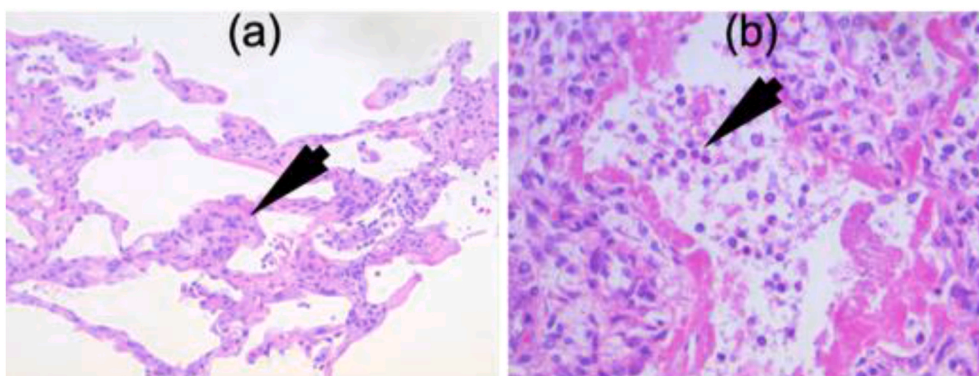
Fig. 15. Microscopic views of (a) interstitial pneumonia and (b) COVID-19 pneumonia. (Courtesy of Luca Saba, A.O.U., Cagliari, Italy.)

Fig. 16. Three lungs with non-COVID-19 pneumonia (a1, a2, and a3). Three lungs with COVID-19 pneumonia with different COVID-19 severities (b1, b2, and b3). (Courtesy of AtheroPoint™, Roseville, CA, USA; reproduced with permission.)

Fig. 17. Bispectrum analysis of non-COVID-19 pneumonia (NCoP) and COVID-19 pneumonia (CoP). (Courtesy of AtheroPoint™, Roseville, CA, USA; reproduced with permission.)

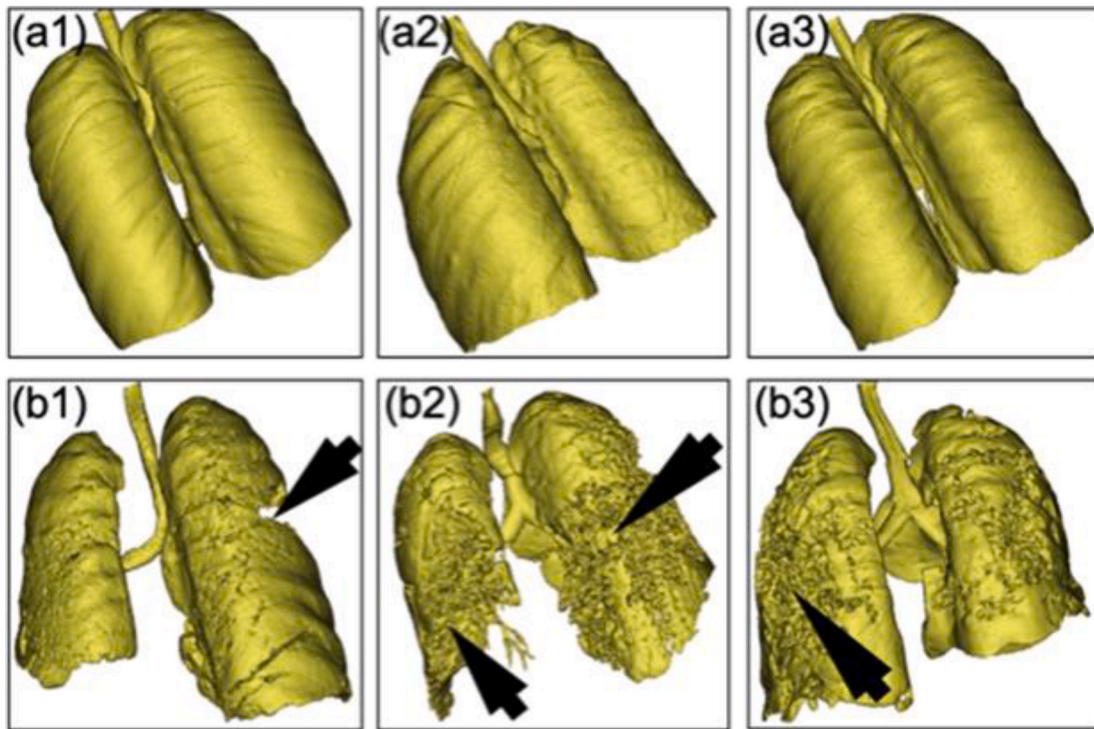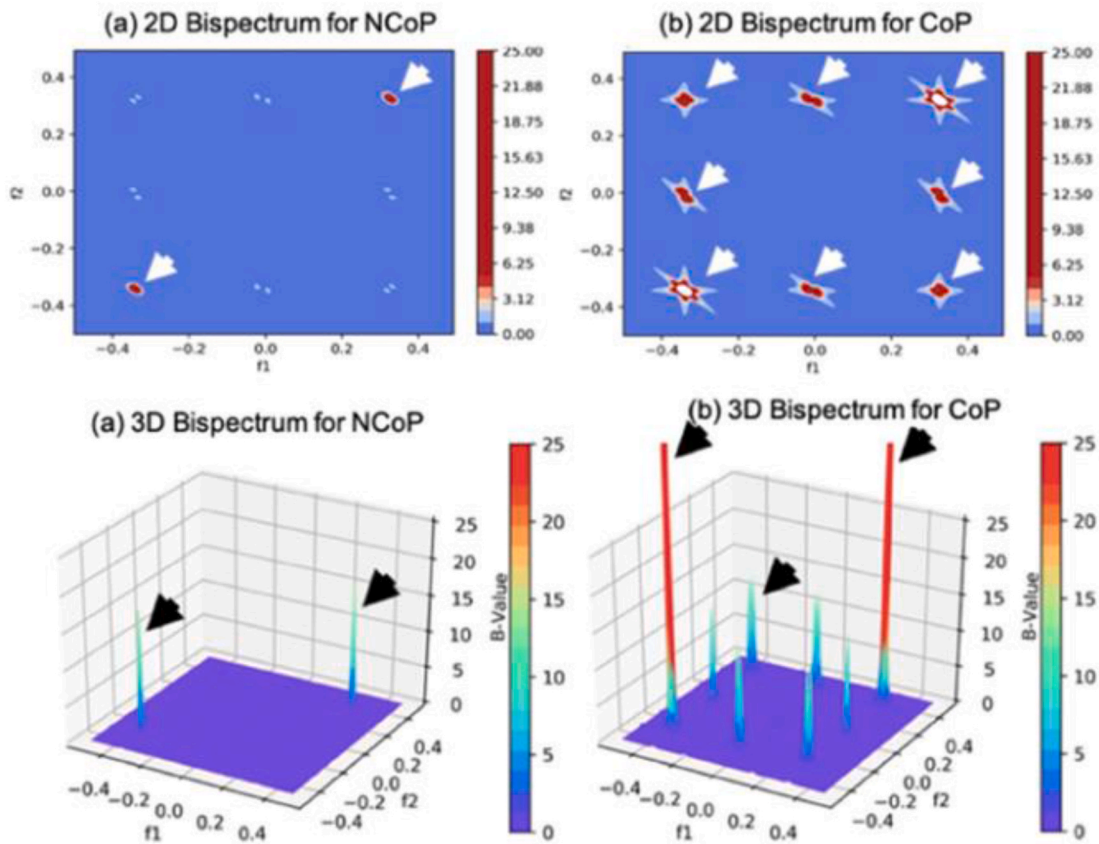among COVID-19 patients. Patient data must also be multiclass, consisting of a control class and various types of pneumonia classes (e.g., COVID-19, viral, bacterial, HIV, and MERS). Meeting these conditions helps to create a more generalized and robust AI system that can be used for COVID-19 diagnostics in any medical setting without the need to perform localized validations or retraining.

AI and Hardware Constraints. GPUs are essential in DL studies [234, 235]. Most of the studies (training and testing) are performed on GPUs using open-source platforms like Google-Colab, with Python as the language and TensorFlow or PyTorch as the framework [14,102].

Strengths, Limitations, and Extensions. This study provides an insight into acute respiratory distress syndrome; into its relationship to co-morbidity; into medical imaging modalities for imaging COVID-19 subjects in an ARDS framework; into the workflow and practical aspects of premier imaging tools; into the design of AI architectures and their adaptation to handle ARDS-based lung severity diagnoses; and finally, into the role of AI-based solutions for comorbid conditions. The study also highlights the critical components needed for a safe and effective AI-based paradigm for risk assessment of COVID-19 severity.

Even though the study offers several new directions through the amalgamation of comorbidity-based AI designs, it is missing several other facets that could be included in a more compressive review. These include the biological processes that inherit comorbidities. This omission is mainly due to limitations of manuscript length. More stringent comparisons of deep learning paradigms can be adapted; we have provided leads to previously published dedicated reviews on AI.

Future research should look for a way to quickly determine the COVID-19 severity using a global positioning system in target lung regions in 2-D and 3-D images, while considering comorbidity and time constraints [236–238]. This fundamental study can also be further developed in several other directions, covering the fields of neurology [239], cardiology, diabetology [240], and ophthalmology [241]. This includes the applications of statistical tools for more systematic review and meta-analysis (SRMA). Since this is a narrative review, the SRMA is beyond its scope.

8. Conclusion

This study is one of the latest contributions that investigated different kinds of comorbidities, its contributions to the ARDS-based framework, its effect on mortality, and finally, the study proposed the AI-based solutions using comorbidity as an independent factor in their design. The salient features of the seven types of school-of-thought were presented, and their architectural characteristics were highlighted. We conclude that there are critical components of the AI system that must be thoroughly investigated before it can be applied clinically for diagnosis of COVID-19 severity. These include (a) scientific and clinical validation, (b) optimization of layers vs. augmentation for best AI optimized architecture design, (c) application of imaging modality based on COVID-19 symptoms severity and troponin release. Lastly, we conclude that the most powerful paradigm where the future holds for ARDS characterization is by incorporating the comorbidity and age-group as one of the distinguishing and novel features in the AI design [242–244].

Declaration of competing interest

We wish to confirm that there are no known conflicts of interest associated with this publication and there has been no significant financial support for this work that could have influenced its outcome. We confirm that the manuscript has been read and approved by all named authors and that there are no other persons who satisfied the criteria for authorship but are not listed. We further confirm that the order of authors listed in the manuscript has been approved by all of us.

We confirm that we have given due consideration to the protection of intellectual propertyassociated with this work and that there are no impediments to publication, including thetiming of publication, with

respect to intellectual property. In so doing we confirm that we have followed the regulations of our institutions concerning intellectual property.

We understand that the Corresponding Author is the sole contact for the Editorial process. He is responsible for communicating with the other authors about progress, submissions of revisions and final approval of proofs. We confirm that we have provided a current, correct email address which is accessible by the Corresponding Author and which has been configured to accept email from."

I, Mainak Biswas on behalf of all authors of the manuscript "A Narrative Review on Characterization of Acute Respiratory Distress Syndrome in COVID-19 Lungs using Artificial Intelligence" hereby declare that the details furnished above are true and correct to the best of my knowledge and belief. In case any of the above information is found to be false or untrue or misleading or misrepresenting, I am aware that I may be held liable for it.

References

[1] M.A. Shereen, S. Khan, A. Kazmi, N. Bashir, R. Siddique, COVID-19 infection: origin, transmission, and characteristics of human coronaviruses, J. Adv. Res. 24 (2020) 91–98.

[2] Y.-R. Guo, Q.-D. Cao, Z.-S. Hong, Y.-Y. Tan, S.-D. Chen, H.-J. Jin, K.-S. Tan, D.-Y. Wang, Y. Yan, The origin, transmission and clinical therapies on coronavirus disease 2019 (COVID-19) outbreak - an update on the status, Mil Med Res 7 (2020), 11-11.

[3] R.J.L. Horton, Offline: COVID-19 is not a pandemic 396 (2020) 874.

[4] D. Cucinotta, M. Vanelli, WHO Declares COVID-19 a Pandemic.

[5] https://www.worldometers.info/coronavirus/.

[6] M. D'Arienzo, A. Coniglio, Assessment of the SARS-CoV-2 basic reproduction number, R (0), based on the early phase of COVID-19 outbreak in Italy, Biosaf Health 2 (2020) 57–59.

[7] S. Ravalli, G. Musumeci, Coronavirus Outbreak in Italy: Physiological Benefits of Home-Based Exercise during Pandemic, Multidisciplinary Digital Publishing Institute, 2020.

[8] A. Wilder-Smith, C.J. Chiew, V.J. Lee, Can we contain the COVID-19 outbreak with the same measures as for SARS? Lancet Infect. Dis. 20 (2020) e102–e107.

[9] G. Maugeri, P. Castrogiovanni, G. Battaglia, R. Pippi, V. D'Agata, A. Palma, M. Di Rosa, G.J.H. Musumeci, The Impact of Physical Activity on Psychological Health during Covid-19 Pandemic in Italy, vol. 6, 2020, e04315.

[10] I.A. Lesser, C.P. Nienhuis, P. Health, The Impact of COVID-19 on Physical Activity Behavior and Well-Being of Canadians, vol. 17, 2020, p. 3899.

[11] V. Viswanathan, A. Puvvula, A.D. Jamthikar, A Pathophysiological Bidirectional Association between Diabetes Mellitus and COVID-19 Leading to Heart and Brain Injury: A Mini-Review.

[12] L. Saba, C. Gerosa, M. Wintermark, U. Hedin, D. Fanni, J.S. Suri, A. Balestrieri, G. Faa, Can COVID19 trigger the plaque vulnerability—a Kounis syndrome warning for "asymptomatic subjects", Cardiovasc. Diagn. Ther. 10 (2020) 1352–1355.

[13] Pubmed COVID-19 Publicatons.

[14] S.S. Skandha, S.K. Gupta, L. Saba, V.K. Koppula, A.M. Johri, N.N. Khanna, S. Mavrogeni, J.R. Laird, G. Pareek, M. Miner, P.P. Sfikakis, A. Protogerou, D. P. Misra, V. Agarwal, A.M. Sharma, V. Viswanathan, V.S. Rathore, M. Turk, R. Kolluri, K. Viskovic, E. Cuadrado-Godia, G.D. Kitas, A. Nicolaides, J.S. Suri, 3-D optimized classification and characterization artificial intelligence paradigm for cardiovascular/stroke risk stratification using carotid ultrasound-based delineated plaque: atheromatic™ 2.0, Comput. Biol. Med. 125 (2020) 103958.

[15] https://ourworldindata.org/grapher/total-confirmed-cases-of-covid-19-per-million-people.

[16] L. Saba, M. Biswas, V. Kuppili, E. Cuadrado Godia, H.S. Suri, D.R. Edla, T. Omerzu, J.R. Laird, N.N. Khanna, S. Mavrogeni, A. Protogerou, P.P. Sfikakis, V. Viswanathan, G.D. Kitas, A. Nicolaides, A. Gupta, J.S. Suri, The present and future of deep learning in radiology, Eur. J. Radiol. 114 (2019) 14–24.

[17] M. Biswas, V. Kuppili, L. Saba, D.R. Edla, H.S. Suri, E. Cuadrado-Godia, J.R. Laird, R.T. Marinhoe, J.M. Sanches, A. Nicolaides, J.S. Suri, State-of-the-art review on deep learning in medical imaging, Front. Biosci. 24 (2019) 392–426.

[18] J.S. Suri, A. Puvvula, M. Biswas, M. Majhail, L. Saba, G. Faa, I.M. Singh, R. Oberleitner, M. Turk, P.S. Chadha, A.M. Johri, J.M. Sanches, N.N. Khanna, K. Viskovic, S. Mavrogeni, J.R. Laird, G. Pareek, M. Miner, D.W. Sobel, A. Balestrieri, P.P. Sfikakis, G. Tsoulfas, A. Protogerou, D.P. Misra, V. Agarwal, G. D. Kitas, P. Ahluwalia, R. Kolluri, J. Teji, M.A. Maini, A. Agbakoba, S.K. Dhanjil, M. Sockalingam, A. Saxena, A. Nicolaides, A. Sharma, V. Rathore, J.N. A. Ajuluchukwu, M. Fatemi, A. Alizad, V. Viswanathan, P.R. Krishnan, S. Naidu, COVID-19 pathways for brain and heart injury in comorbidity patients: a role of medical imaging and artificial intelligence-based COVID severity classification: a review, Comput. Biol. Med. 124 (2020), 103960-103960.

[19] M. Gatto, E. Bertuzzo, L. Mari, S. Miccoli, L. Carraro, R. Casagrandi, A. Rinaldo, Spread and dynamics of the COVID-19 epidemic in Italy: effects of emergency containment measures, Proc. Natl. Acad. Sci. U. S. A. 117 (2020) 10484–10491.

[20] S.J.C. rekha Hanumanthu, Solitons, Fractals, Role of Intelligent Computing in COVID-19 Prognosis: A State-Of-The-Art Review, 2020, p. 109947.

[21] Y. Deng, L. Lei, Y. Chen, W. Zhang, The potential added value of FDG PET/CT for COVID-19 pneumonia, Eur. J. Nucl. Med. Mol. Imag. 47 (2020) 1634–1635.

[22] C. Liu, J. Zhou, L. Xia, X. Cheng, D. Lu, 18F-FDG PET/CT and serial chest CT findings in a COVID-19 patient with dynamic clinical characteristics in different period, Clin. Nucl. Med. 45 (2020) 495–496.

[23] S. Maurea, C.G. Mainolfi, C. Bombace, A. Annunziata, L. Attanasio, M. Petretta, S. Del Vecchio, A. Cuocolo, FDG-PET/CT imaging during the Covid-19 emergency: a southern Italian perspective, Eur. J. Nucl. Med. Mol. Imag. 47 (2020) 2691–2697.

[24] P. Verdecchia, C. Cavallini, A. Spanevello, F. Angeli, The pivotal link between ACE2 deficiency and SARS-CoV-2 infection, Eur. J. Intern. Med. 76 (2020) 14–20.

[25] E.C. Mossel, J. Wang, S. Jeffers, K.E. Edeen, S. Wang, G.P. Cosgrove, C.J. Funk, R. Manzer, T.A. Miura, L.D. Pearson, K.V. Holmes, R.J. Mason, SARS-CoV replicates in primary human alveolar type II cell cultures but not in type I-like cells, Virology 372 (2008) 127–135.

[26] Luca Saba, D.F. Clara Gerosa, Francesco Marongiu, Giorgio La Nasa, Giovanni Caocci, Doris Barcellona, Antonella Balestrieri, Ferdinando Coghe, Germano Orru, S Suri Jasjit, Riccardo Cau, Massimo Castagnola, Gavino Faa, Molecular Pathways Triggered by COVID19 in Different Organs: ACE2 Receptor-Expressing Cells under Attack? A Review, 2020.

[27] P. Zhou, X.-L. Yang, X.-G. Wang, B. Hu, L. Zhang, W. Zhang, H.-R. Si, Y. Zhu, B. Li, C.-L. Huang, H.-D. Chen, J. Chen, Y. Luo, H. Guo, R.-D. Jiang, M.-Q. Liu, Y. Chen, X.-R. Shen, X. Wang, X.-S. Zheng, K. Zhao, Q.-J. Chen, F. Deng, L.-L. Liu, B. Yan, F.-X. Zhan, Y.-Y. Wang, G.-F. Xiao, Z.-L. Shi, A pneumonia outbreak associated with a new coronavirus of probable bat origin, Nature 579 (2020) 270–273.

[28] Z. Qian, E.A. Travanty, L. Oko, K. Edeen, A. Berglund, J. Wang, Y. Ito, K. V. Holmes, R.J. Mason, Innate immune response of human alveolar type II cells infected with severe acute respiratory syndrome-coronavirus, Am. J. Respir. Cell Mol. Biol. 48 (2013) 742–748.

[29] Y. Ding, H. Wang, H. Shen, Z. Li, J. Geng, H. Han, J. Cai, X. Li, W. Kang, D. Weng, Y. Lu, D. Wu, L. He, K. Yao, The clinical pathology of severe acute respiratory syndrome (SARS): a report from China, J. Pathol. 200 (2003) 282–289.

[30] J. Liu, X. Zheng, Q. Tong, W. Li, B. Wang, K. Sutter, M. Trilling, M. Lu, U. Dittmer, D. Yang, Overlapping and discrete aspects of the pathology and pathogenesis of the emerging human pathogenic coronaviruses SARS-CoV, MERS-CoV, and 2019-nCoV, J. Med. Virol. 92 (2020) 491–494.

[31] S. Wang, T.Q. Le, N. Kurihara, J. Chida, Y. Cisse, M. Yano, H. Kido, Influenza virus-cytokine-protease cycle in the pathogenesis of vascular hyperpermeability in severe influenza, J. Infect. Dis. 202 (2010) 991–1001.

[32] C. Huang, Y. Wang, X. Li, L. Ren, J. Zhao, Y. Hu, L. Zhang, G. Fan, J. Xu, X. Gu, Z. Cheng, T. Yu, J. Xia, Y. Wei, W. Wu, X. Xie, W. Yin, H. Li, M. Liu, Y. Xiao, H. Gao, L. Guo, J. Xie, G. Wang, R. Jiang, Z. Gao, Q. Jin, J. Wang, B. Cao, Clinical features of patients infected with 2019 novel coronavirus in Wuhan, China, Lancet 395 (2020) 497–506.

[33] M.A. Matthay, L.B. Ware, G.A. Zimmerman, The acute respiratory distress syndrome, J. Clin. Invest. 122 (2012) 2731–2740.

[34] A.L. Katzenstein, C.M. Bloor, A.A. Leibow, Diffuse alveolar damage–the role of oxygen, shock, and related factors. A review, Am. J. Pathol. 85 (1976) 209–228.

[35] T.J. Nuckton, J.A. Alonso, R.H. Kallet, B.M. Daniel, J.-F. Pittet, M.D. Eisner, M. A. Matthay, Pulmonary dead-space fraction as a risk factor for death in the acute respiratory distress syndrome, N. Engl. J. Med. 346 (2002) 1281–1286.

[36] C. Wu, X. Chen, Y. Cai, J.a. Xia, X. Zhou, S. Xu, H. Huang, L. Zhang, X. Zhou, C. Du, Y. Zhang, J. Song, S. Wang, Y. Chao, Z. Yang, J. Xu, X. Zhou, D. Chen, W. Xiong, L. Xu, F. Zhou, J. Jiang, C. Bai, J. Zheng, Y. Song, Risk factors associated with acute respiratory distress syndrome and death in patients with coronavirus disease 2019 pneumonia in wuhan, China, JAMA Intern Med 180 (2020) 934–943.

[37] J. Lian, X. Jin, S. Hao, H. Cai, S. Zhang, L. Zheng, H. Jia, J. Hu, J. Gao, Y. Zhang, X. Zhang, G. Yu, X. Wang, J. Gu, C. Ye, C. Jin, Y. Lu, X. Yu, X. Yu, Y. Ren, Y. Qiu, L. Li, J. Sheng, Y. Yang, Analysis of epidemiological and clinical features in older patients with coronavirus disease 2019 (COVID-19) outside wuhan, Clin. Infect. Dis. 71 (2020) 740–747.

[38] Y. Liu, W. Sun, J. Li, L. Chen, Y. Wang, L. Zhang, L. Yu, Clinical Features and Progression of Acute Respiratory Distress Syndrome in Coronavirus Disease 2019, Cold Spring Harbor Laboratory, 2020.

[39] A. Khan, A. Chatterjee, S. Singh, Comorbidities and Disparities in Outcomes of COVID-19 Among African American and White Patients, Cold Spring Harbor Laboratory, 2020.

[40] P. Zhang, L. Zhu, J. Cai, F. Lei, J.-J. Qin, J. Xie, Y.-M. Liu, Y.-C. Zhao, X. Huang, L. Lin, M. Xia, M.-M. Chen, X. Cheng, X. Zhang, D. Guo, Y. Peng, Y.-X. Ji, J. Chen, Z.-G. She, Y. Wang, Q. Xu, R. Tan, H. Wang, J. Lin, P. Luo, S. Fu, H. Cai, P. Ye, B. Xiao, W. Mao, L. Liu, Y. Yan, M. Liu, M. Chen, X.-J. Zhang, S. Wang, M. Touyz Rhian, J. Xia, B.-H. Zhang, X. Huang, Y. Yuan, R. Loomba, P. Liu Peter, H. Li, Association of inpatient use of angiotensin-converting enzyme inhibitors and angiotensin II receptor blockers with mortality among patients with hypertension hospitalized with COVID-19, Circ. Res. 126 (2020) 1671–1681.

[41] M. Maniruzzaman, N. Kumar, M. Menhazul Abedin, M. Shaykhul Islam, H.S. Suri, A.S. El-Baz, J.S. Suri, Comparative approaches for classification of diabetes mellitus data: machine learning paradigm, Comput. Methods Progr. Biomed. 152 (2017) 23–34.

[42] M. Dreher, A. Kersten, J. Bickenbach, P. Balfanz, B. Hartmann, C. Cornelissen, A. Daher, R. Stöhr, M. Kleines, S.W. Lemmen, J.C. Brokmann, T. Müller, D. Müller-Wieland, G. Marx, N. Marx, The characteristics of 50 hospitalized

[43] L. Palaiodimos, D.G. Kokkinidis, W. Li, D. Karamanis, J. Ognibene, S. Arora, W. N. Southern, C.S. Mantzoros, Severe obesity, increasing age and male sex are independently associated with worse in-hospital outcomes, and higher in-hospital mortality, in a cohort of patients with COVID-19 in the Bronx, New York, Metabolism 108 (2020), 154262-154262.

[44] T. Yu, S. Cai, Z. Zheng, X. Cai, Y. Liu, S. Yin, J. Peng, X. Xu, Association between clinical manifestations and prognosis in patients with COVID-19, Clin. Therapeut. 42 (2020) 964–972.

[45] D. Bandyopadhyay, T. Akhtar, A. Hajra, M. Gupta, A. Das, S. Chakraborty, I. Pal, N. Patel, B. Amgai, R.K. Ghosh, G.C. Fonarow, C.J. Lavie, S.S. Naidu, COVID-19 pandemic: cardiovascular complications and future implications, Am. J. Cardiovasc. Drugs: Drugs, Devices, and other Interventions 20 (2020) 311–324.

[46] D. Doyen, P. Moceri, D. Ducreux, J. Dellamonica, Myocarditis in a patient with COVID-19: a cause of raised troponin and ECG changes, Lancet 395 (2020) 1516.

[47] M. Madjid, P. Safavi-Naeini, S.D. Solomon, O. Vardeny, Potential effects of coronaviruses on the cardiovascular system: a review, JAMA Cardiol 5 (2020) 831–840.

[48] G. Suleyman, R.A. Fadel, K.M. Malette, C. Hammond, H. Abdulla, A. Entz, Z. Demertzis, Z. Hanna, A. Failla, C. Dagher, Z. Chaudhry, A. Vahia, O. Abreu Lanfranco, M. Ramesh, M.J. Zervos, G. Alangaden, J. Miller, I. Brar, Clinical characteristics and morbidity associated with coronavirus disease 2019 in a series of patients in metropolitan detroit, JAMA Netw Open 3 (2020), e2012270.

[49] E.A. Meyerowitz, A.Y. Kim, K.L. Ard, N. Basgoz, J.T. Chu, R.M. Hurtado, C.K. Lee, W. He, T. Minukas, S. Nelson, B.O. Ojikutu, G. Robbins, S. Sanchez, V.A. Triant, K. Zachary, R.T. Gandhi, Disproportionate burden of coronavirus disease 2019 among racial minorities and those in congregate settings among a large cohort of people with HIV, AIDS 34 (2020) 1781–1787.

[50] M. Chandran, A. Chan Maung, A. Mithal, R. Parameswaran, Vitamin D in COVID - 19: dousing the fire or averting the storm? – a perspective from the Asia-Pacific, Osteoporosis and Sarcopenia 6 (2020) 97–105.

[51] T.S. Chang, Y. Ding, M.K. Freund, R. Johnson, T. Schwarz, J.M. Yabu, C. Hazlett, J.N. Chiang, A. Wulf, D.H. Geschwind, M.J. Butte, B. Pasaniuc, Prior Diagnoses and Medications as Risk Factors for COVID-19 in a Los Angeles Health System, medRxiv, 2020.

[52] A. Sanyaolu, C. Okorie, A. Marinkovic, R. Patidar, K. Younis, P. Desai, Z. Hosein, I. Padda, J. Mangat, M. Altaf, Comorbidity and its impact on patients with COVID-19, SN Compr Clin Med (2020) 1–8.

[53] M. Takemoto, M.O. Menezes, C.B. Andreucci, R. Knobel, L. Sousa, L. Katz, E. B. Fonseca, M. Nakamura-Pereira, C.G. Magalhaes, C. Diniz, A. Melo, M. Amorim, C. Brazilian Group for Studies of, Pregnancy, Clinical Characteristics and Risk Factors for Mortality in Obstetric Patients with Severe COVID-19 in Brazil: a Surveillance Database Analysis, BJOG, 2020.

[54] S. Gudipati, I. Brar, S. Murray, J.E. McKinnon, N. Yared, N.J. Markowitz, Descriptive Analysis of Patients Living with HIV Affected by COVID-19, 2020.

[55] S.R. Bornstein, F. Rubino, K. Khunti, G. Mingrone, D. Hopkins, A.L. Birkenfeld, B. Boehm, S. Amiel, R.I.G. Holt, J.S. Skyler, J.H. DeVries, E. Renard, R.H. Eckel, P. Zimmet, K.G. Alberti, J. Vidal, B. Geloneze, J.C. Chan, L. Ji, B. Ludwig, Practical recommendations for the management of diabetes in patients with COVID-19, Lancet Diabet. Endocrinol. 8 (2020) 546–550.

[56] T.J. Guzik, S.A. Mohiddin, A. Dimarco, V. Patel, K. Savvatis, F.M. Marelli-Berg, M. S. Madhur, M. Tomaszewski, P. Maffia, F. D'Acquisto, S.A. Nicklin, A.J. Marian, R. Nosalski, E.C. Murray, B. Guzik, C. Berry, R.M. Touyz, R. Kreutz, D.W. Wang, D. Bhella, O. Sagliocco, F. Crea, E.C. Thomson, I.B. McInnes, COVID-19 and the cardiovascular system: implications for risk assessment, diagnosis, and treatment options, Cardiovasc. Res. 116 (2020) 1666–1687.

[57] M.F. Bassendine, S.H. Bridge, G.W. McCaughan, M.D. Gorrell, COVID-19 and comorbidities: a role for dipeptidyl peptidase 4 (DPP4) in disease severity? J. Diabetes 12 (2020) 649–658.

[58] B. Bode, V. Garrett, J. Messler, R. McFarland, J. Crowe, R. Booth, D.C. Klonoff, Glycemic characteristics and clinical outcomes of COVID-19 patients hospitalized in the United States, J Diabet. Sci Technol 14 (2020) 813–821.

[59] J. Akram, S. Azhar, M. Shahzad, W. Latif, K.S. Khan, Pakistan Randomized and Observational Trial to Evaluate Coronavirus Treatment (PROTECT) of Hydroxychloroquine, Oseltamivir and Azithromycin to treat newly diagnosed patients with COVID-19 infection who have no comorbidities like diabetes mellitus: a structured summary of a study protocol for a randomized controlled trial, Trials 21 (2020) 702.

[60] Q. Yang, L. Xie, W. Zhang, L. Zhao, H. Wu, J. Jiang, J. Zou, J. Liu, J. Wu, Y. Chen, J. Wu, Analysis of the clinical characteristics, drug treatments and prognoses of 136 patients with coronavirus disease 2019, J. Clin. Pharm. Therapeut. 45 (2020) 609–616.

[61] M. Halaji, A. Farahani, R. Ranjbar, M. Heiat, F.J. Dehkordi, Emerging Coronaviruses: First SARS, Second MERS and Third SARS-CoV-2: Epidemiological Updates of COVID-19, vol. 28, 2020, pp. 6–17.

[62] D. Grimaldi, N. Aissaoui, G. Blonz, G. Carbutti, R. Courcelle, S. Gaudry, A. Gaultier, A. D'Hondt, J. Higny, G. Horlait, S. Hraiech, L. Lefebvre, F. Lejeune, A. Ly, M. Piagnerelli, B. Sauneuf, N. Serck, T. Soumagne, P. Szychowiak, J. Textoris, B. Vandenbunder, C. Vinsonneau, J.B. Lascarrou, C.s. group, Characteristics and outcomes of acute respiratory distress syndrome related to COVID-19 in Belgian and French intensive care units according to antiviral strategies: the COVADIS multicentre observational study, Ann. Intensive Care 10 (2020) 131.

[63] S. Zaim, J.H. Chong, V. Sankaranarayanan, A. Harky, COVID-19 and multiorgan response, Curr. Probl. Cardiol. 45 (2020) 100618.

[64] F.R. Ponziani, F. Del Zompo, A. Nesci, F. Santopaolo, G. Ianiro, M. Pompili, A. Gasbarrini, C.-g. Gemelli against, Liver involvement is not associated with mortality: results from a large cohort of SARS-CoV-2 positive patients, Aliment. Pharmacol. Ther. 52 (6) (2020) 1060–1068.

[65] J.S. Brandt, J. Hill, A. Reddy, M. Schuster, H.S. Patrick, T. Rosen, M.V. Sauer, C. Boyle, C.V. Ananth, Epidemiology of coronavirus disease 2019 in pregnancy: risk factors and associations with adverse maternal and neonatal outcomes, Am. J. Obstet. Gynecol. (2020).

[66] L.L. Cheng, W.J. Guan, C.Y. Duan, N.F. Zhang, C.L. Lei, Y. Hu, A.L. Chen, S.Y. Li, C. Zhuo, X.L. Deng, F.J. Cheng, Y. Gao, J.H. Zhang, J.X. Xie, H. Peng, Y.X. Li, X. W. Wu, W. Liu, H. Peng, J. Wang, G.M. Xiao, P.Y. Chen, C.Y. Wang, Z.F. Yang, J. C. Zhao, N.S. Zhong, Effect of recombinant human granulocyte colony-stimulating factor for patients with coronavirus disease 2019 (COVID-19) and lymphopenia: a randomized clinical trial, JAMA Intern Med 181 (1) (2021) 71–78.

[67] M.J. Cummings, M.R. Baldwin, D. Abrams, S.D. Jacobson, B.J. Meyer, E. M. Balough, J.G. Aaron, J. Claassen, L.E. Rabbani, J. Hastie, B.R. Hochman, J. Salazar-Schicchi, N.H. Yip, D. Brodie, M.R. O'Donnell, Epidemiology, clinical course, and outcomes of critically ill adults with COVID-19 in New York City: a prospective cohort study, Lancet 395 (2020) 1763–1770.

[68] M. Nakeshbandi, R. Maini, P. Daniel, S. Rosengarten, P. Parmar, C. Wilson, J. M. Kim, A. Oommen, M. Mecklenburg, J. Salvani, M.A. Joseph, I. Breitman, The impact of obesity on COVID-19 complications: a retrospective cohort study, Int. J. Obes. 44 (2020) 1832–1837.

[69] J. Zhao, X. Li, Y. Gao, W.J. Huang, Risk factors for the exacerbation of patients with 2019 Novel Coronavirus, A Meta Analysis 17 (2020) 1744.

[70] T. Chen, D. Wu, H. Chen, W. Yan, D. Yang, G. Chen, K. Ma, D. Xu, H. Yu, H. Wang, T. Wang, W. Guo, J. Chen, C. Ding, X. Zhang, J. Huang, M. Han, S. Li, X. Luo, J. Zhao, Q. Ning, Clinical Characteristics of 113 Deceased Patients with Coronavirus Disease 2019: Retrospective Study, Bmj, 2020.

[71] C. Qin, L. Zhou, Z. Hu, S. Yang, S. Zhang, M. Chen, H. Yu, D.S. Tian, W. Wang, Clinical characteristics and outcomes of COVID-19 patients with a history of stroke in wuhan, China, Stroke 51 (2020) 2219–2223.

[72] S. Shi, M. Qin, B. Shen, Y. Cai, T. Liu, F. Yang, W. Gong, X. Liu, J. Liang, Q. Zhao, H. Huang, B. Yang, C. Huang, Association of cardiac injury with mortality in hospitalized patients with COVID-19 in wuhan, China, JAMA Cardiol 5 (2020) 802–810.

[73] Y. Deng, W. Liu, K. Liu, Y.Y. Fang, J. Shang, L. Zhou, K. Wang, F. Leng, S. Wei, L. Chen, H.G. Liu, Clinical characteristics of fatal and recovered cases of coronavirus disease 2019 in Wuhan, China: a retrospective study, Chin Med J (Engl) 133 (2020) 1261–1267.

[74] F. Yang, S. Shi, J. Zhu, J. Shi, K. Dai, X. Chen, Clinical characteristics and outcomes of cancer patients with COVID-19, J. Med. Virol. 92 (10) (2020) 2067–2073.

[75] F. Del Sole, A. Farcomeni, L. Loffredo, R. Carnevale, D. Menichelli, T. Vicario, P. Pignatelli, D. Pastori, Features of severe COVID-19: a systematic review and meta-analysis, Eur. J. Clin. Invest. 50 (2020) e13378-e13378.

[76] F. Ciceri, A. Castagna, P. Rovere-Querini, F. De Cobelli, A. Ruggeri, L. Galli, C. Conte, R. De Lorenzo, A. Poli, A. Ambrosio, C. Signorelli, E. Bossi, M. Fazio, C. Tresoldi, S. Colombo, G. Monti, E. Fominskiy, S. Franchini, M. Spessot, C. Martinenghi, M. Carlucci, L. Beretta, A.M. Scandroglio, M. Clementi, M. Locatelli, M. Tresoldi, P. Scarpellini, G. Martino, E. Bosi, L. Dagna, A. Lazzarin, G. Landoni, A. Zangrillo, Early predictors of clinical outcomes of COVID-19 outbreak in Milan, Italy, Clin. Immunol. 217 (2020) 108509.

[77] M.A. Kutluhan, A. Taş, A. Şahin, A. Ürkmez, R. Topaktas, Ö. Ataç, A.J. Verit, Assessment of Clinical Features and Renal Functions in Coronavirus Disease-19: A Retrospective Analysis of 96 Patients, 2020, e13636.

[78] K.R. Derespina, S. Kaushik, A. Plichta, E.E. Conway Jr., A. Bercow, J. Choi, R. Eisenberg, J. Gillen, A.I. Sen, C.M.J. Hennigan, Clinical Manifestations and Outcomes of Critically Ill Children and Adolescents with Coronavirus Disease 2019 in New York City, 2020.

[79] E. Blumfield, T.L.J.P.r. Levin, COVID-19 in Pediatric Patients: a Case Series from the Bronx, NY, vol. 50, 2020, pp. 1369–1374.

[80] A.-R. Jazieh, T.H. Alenazi, A. Alhejazi, F. Al Safi, A.J.J.G.O. Al Olayan, Outcome of Oncology Patients Infected with Coronavirus, vol. 6, 2020, pp. 471–475.

[81] K. Al-Wahaibi, Y. Al-Wahshi, O. Mohamed Elfadil, Myocardial injury is associated with higher morbidity and mortality in patients with 2019 novel coronavirus disease (COVID-19), SN Compr Clin Med (2020) 1–7.

[82] S. Chand, S. Kapoor, D. Orsi, M.J. Fazzari, T.G. Tanner, G.C. Umeh, M. Islam, P. V. Dicpinigaitis, COVID-19-Associated critical illness-report of the first 300 patients admitted to intensive care units at a New York city medical center, J. Intensive Care Med. 35 (2020) 963–970.

[83] Y.R. Lee, M.K. Kang, J.E. Song, H.J. Kim, Y.O. Kweon, W.Y. Tak, S.Y. Jang, J. G. Park, C. Lee, J.S. Hwang, B.K. Jang, J.I. Suh, W.J. Chung, B.S. Kim, S.Y. Park, Clinical outcomes of coronavirus disease 2019 in patients with pre-existing liver diseases: a multicenter study in South Korea, Clin. Mol. Hepatol. 26 (2020) 562–576.

[84] L. Wang, W. He, X. Yu, D. Hu, M. Bao, H. Liu, J. Zhou, H. Jiang, Coronavirus disease 2019 in elderly patients: characteristics and prognostic factors based on 4-week follow-up, J. Infect. 80 (2020) 639–645.

[85] Y. Du, L. Tu, P. Zhu, M. Mu, R. Wang, P. Yang, X. Wang, C. Hu, R. Ping, P. Hu, T. Li, F. Cao, C. Chang, Q. Hu, Y. Jin, G. Xu, Clinical features of 85 fatal cases of COVID-19 from wuhan. A retrospective observational study, Am. J. Respir. Crit. Care Med. 201 (2020) 1372–1379.

[86] D.R. Ziehr, J. Alladina, C.R. Petri, J.H. Maley, A. Moskowitz, B.D. Medoff, K. A. Hibbert, B.T. Thompson, C.C. Hardin, Respiratory pathophysiology of mechanically ventilated patients with COVID-19: a cohort study, Am. J. Respir. Crit. Care Med. 201 (2020) 1560–1564.

[87] E. Garcia-Cruz, D. Manzur-Sandoval, R. Rascon-Sabido, R. Gopar-Nieto, R. L. Barajas-Campos, A. Jordan-Rios, D. Sierra-Lara Martinez, G.M. Jimenez-Rodriguez, A.L. Murillo-Ochoa, A. Diaz-Mendez, E. Lazcano-Diaz, D. Araiza-Garaygordobil, A. Cabello-Lopez, E. Melano-Carranza, E. Bucio-Reta, F. J. Gonzalez-Ruiz, L.A. Cota-Apodaca, L.E. Santos-Martinez, G. Fernandez-de la Reguera, A. Ramos-Enriquez, G. Rojas-Velasco, R.J. Alvarez-Alvarez, F. Baranda-Tovar, Critical care ultrasonography during COVID-19 pandemic: the ORACLE protocol, Echocardiography 37 (9) (2020) 1353–1361.

[88] Y. Huang, H. Guo, Y. Zhou, J. Guo, T. Wang, X. Zhao, H. Li, Y. Sun, X. Bian, C. Fang, The associations between fasting plasma glucose levels and mortality of COVID-19 in patients without diabetes, Diabetes Res. Clin. Pract. 169 (2020) 108448.

[89] J. Arrieta, S. Galwankar, N. Lattanzio, D. Ray, A. Agrawal, Studying the clinical data of COVID positive patients admitted to a tertiary care academic hospital, J. Emergencies, Trauma, Shock 13 (2020) 131–134.

[90] M. Oltean, J.M. Søfteland, J. Bagge, J. Ekelund, M. Felldin, A. Schult, J. Magnusson, V. Friman, K.J.I.D. Karason, Covid-19 in Kidney Transplant Recipients: a Systematic Review of the Case Series Available Three Months into the Pandemic, vol. 52, 2020, pp. 830–837.

[91] S. Marinaki, S. Tsiakas, M. Korogiannou, K. Grigorakos, V. Papalois, I.J. Boletis, A systematic review of COVID-19 infection in kidney transplant recipients: a universal effort to preserve patients', Lives and Allografts 9 (2020) 2986.

[92] A. Rajpal, L. Rahimi, F.J.J.o.d. Ismail-Beigi, Factors Leading to High Morbidity and Mortality of COVID-19 in Patients with Type 2 Diabetes, 2020.

[93] I. Huang, M.A. Lim, R. Pranata, Diabetes mellitus is associated with increased mortality and severity of disease in COVID-19 pneumonia - a systematic review, meta-analysis, and meta-regression, Diabet Metab Syndr 14 (2020) 395–403.

[94] M. Salerno, F. Sessa, A. Piscopo, A. Montana, M. Torrisi, F. Patanè, P. Murabito, G.L. Volti, C. Pomara, No autopsies on COVID-19 deaths: a missed opportunity and the lockdown of science, J. Clin. Med. 9 (2020) 1472.

[95] J. Arrieta, S. Galwankar, N. Lattanzio, D. Ray, A. Agrawal, Common clinical characteristics and complications determining the outcome in a COVID-Positive predominantly geriatric population, J. Emergencies, Trauma, Shock 13 (2020).

[96] B.M. Tomazini, I.S. Maia, A.B. Cavalcanti, O. Berwanger, R.G. Rosa, V.C. Veiga, A. Avezum, R.D. Lopes, F.R. Bueno, M.V.A.O. Silva, F.P. Baldassare, E.L.V. Costa, R.A.B. Moura, M.O. Honorato, A.N. Costa, L.P. Damiani, T. Lisboa, L. Kawano-Dourado, F.G. Zampieri, G.B. Olivato, C. Righy, C.P. Amendola, R.M.L. Roepke, D. H.M. Freitas, D.N. Forte, F.G.R. Freitas, C.C.F. Fernandes, L.M.G. Melro, G.F. S. Junior, D.C. Morais, S. Zung, F.R. Machado, L.C.P. Azevedo, C.C.-B. I. Investigators, Effect of dexamethasone on days alive and ventilator-free in patients with moderate or severe acute respiratory distress syndrome and COVID-19: the CoDEX randomized clinical trial, J. Am. Med. Assoc. 324 (2020) 1307–1316.

[97] N. Nasir, J. Farooqi, S.F. Mahmood, K. Jabeen, COVID-19-associated pulmonary aspergillosis (CAPA) in patients admitted with severe COVID-19 pneumonia: an observational study from Pakistan, Mycoses 63 (2020) 766–770.

[98] L. Antoun, N.E. Taweel, I. Ahmed, S. Patni, H. Honest, Maternal COVID-19 infection, clinical characteristics, pregnancy, and neonatal outcome: a prospective cohort study, Eur. J. Obstet. Gynecol. Reprod. Biol. 252 (2020) 559–562.

[99] M. Khan, H. Khan, S. Khan, M. Nawaz, Epidemiological and clinical characteristics of coronavirus disease (COVID-19) cases at a screening clinic during the early outbreak period: a single-centre study, J. Med. Microbiol. 69 (2020) 1114–1123.

[100] J. Xie, Y. Zu, A. Alkhatib, T.T. Pham, F. Gill, A. Jang, S. Radosta, G. Chaaya, L. Myers, J.S. Zifodya, C.M. Bojanowski, N.F. Marrouche, F. Mauvais-Jarvis, J. L. Denson, Metabolic syndrome and COVID-19 mortality among adult black patients in new orleans, Diabetes Care 44 (1) (2020) 188–193.

[101] T. Li, L. Lu, W. Zhang, Y. Tao, L. Wang, J. Bao, B. Liu, J. Duan, Clinical characteristics of 312 hospitalized older patients with COVID-19 in Wuhan, China, Arch. Gerontol. Geriatr. 91 (2020) 104185.

[102] L. Saba, M. Agarwal, S. Sanagala, S. Gupta, G. Sinha, A. Johri, N. Khanna, S. Mavrogeni, J. Laird, G.J.E.L. Pareek, Brain MRI-Based Wilson Disease Tissue Classification: an Optimised Deep Transfer Learning Approach, 2020.

[103] G.S. Tandel, M. Biswas, O.G. Kakde, A. Tiwari, H.S. Suri, M. Turk, J.R. Laird, C. K. Asare, A.A. Ankrah, N.J.C. Khanna, A review on a deep learning perspective in brain cancer classification 11 (2019) 111.

[104] L. Saba, A. Tiwari, M. Biswas, S.K. Gupta, E. Godia-Cuadrado, A. Chaturvedi, M. Turk, H.S. Suri, S. Orru, J.M. Sanches, Wilson's disease: a new perspective review on its genetics, Diagnosis Treatment 11 (2019) 166–185.

[105] U.R. Acharya, M.R.K. Mookiah, S.V. Sree, D. Afonso, J. Sanches, S. Shafique, A. Nicolaides, L.M. Pedro, J.F. e Fernandes, J.S.J.M. Suri, b. engineering, computing, Atherosclerotic plaque tissue characterization in 2D ultrasound longitudinal carotid scans for automated classification, Paradigm Stroke Risk Assess. 51 (2013) 513–523.

[106] A.M. Sharma, A. Gupta, P.K. Kumar, J. Rajan, L. Saba, I. Nobutaka, J.R. Laird, A. Nicolades, J.S. Suri, A Review on Carotid Ultrasound Atherosclerotic Tissue Characterization and Stroke Risk Stratification in Machine Learning Framework, vol. 17, 2015, p. 55.

[107] M. Biswas, V. Kuppili, L. Saba, D.R. Edla, H.S. Suri, A. Sharma, E. Cuadrado-Godia, J.R. Laird, A. Nicolaides, J.S.J.M. Suri, b. engineering, computing, Deep learning fully convolution network for lumen characterization in diabetic patients using carotid ultrasound: a tool for stroke risk 57 (2019) 543–564.

[108] L. Saba, P.K. Jain, H.S. Suri, N. Ikeda, T. Araki, B.K. Singh, A. Nicolaides, S. Shafique, A. Gupta, J.R. Laird, Plaque Tissue Morphology-Based Stroke Risk Stratification Using Carotid Ultrasound: a Polling-Based PCA Learning Paradigm, vol. 41, 2017, p. 98.

[109] U. Acharya, S.V. Sree, M. Mookiah, L. Saba, H. Gao, G. Mallarini, J.J. Suri, Part H: journal of Engineering in Medicine, Computed tomography carotid wall plaque characterization using a combination of discrete wavelet transform and texture features, A pilot Study 227 (2013) 643–654.

[110] U.R. Acharya, F. Molinari, L. Saba, A. Nicolaides, S. Shafique, J.S. Suri, Carotid ultrasound symptomatology using atherosclerotic plaque characterization: a class of Atheromatic systems, in: 2012 Annual International Conference of the IEEE Engineering in Medicine and Biology Society, IEEE, 2012, pp. 3199–3202.

[111] H. Prasad, R.J. Martis, U.R. Acharya, L.C. Min, J.S. Suri, Application of higher order spectra for accurate delineation of atrial arrhythmia, in: 2013 35th Annual International Conference of the IEEE Engineering in Medicine and Biology Society (EMBC), IEEE, 2013, pp. 57–60.

[112] L. Saba, N. Dey, A.S. Ashour, S. Samanta, S.S. Nath, S. Chakraborty, J. Sanches, D. Kumar, R. Marinho, J.S.J.C.m. Suri, p.i. biomedicine, Automated Stratification of Liver Disease in Ultrasound: an Online Accurate Feature Classification Paradigm, vol. 130, 2016, pp. 118–134.

[113] U.R. Acharya, S.V. Sree, R. Ribeiro, G. Krishnamurthi, R.T. Marinho, J. Sanches, J.S.J.M.p. Suri, Data Mining Framework for Fatty Liver Disease Classification in Ultrasound: a Hybrid Feature Extraction Paradigm, vol. 39, 2012, pp. 4255–4264.

[114] M. Biswas, V. Kuppili, D.R. Edla, H.S. Suri, L. Saba, R.T. Marinhoe, J.M. Sanches, J.S.J.C.m. Suri, p.i. Biomedicine, Symtosis: A Liver Ultrasound Tissue Characterization and Risk Stratification in Optimized Deep Learning Paradigm, vol. 155, 2018, pp. 165–177.

[115] A. Boi, A.D. Jamthikar, L. Saba, D. Gupta, A. Sharma, B. Loi, J.R. Laird, N. N. Khanna, J.S. Suri, A Survey on Coronary Atherosclerotic Plaque Tissue Characterization in Intravascular Optical Coherence Tomography, vol. 20, 2018, p. 33.

[116] U.R. Acharya, O. Faust, N.A. Kadri, J.S. Suri, W.J.C.i.b. Yu, Medicine, Automated Identification of Normal and Diabetes Heart Rate Signals Using Nonlinear Measures, vol. 43, 2013, pp. 1523–1529.

[117] G. Pareek, U.R. Acharya, S.V. Sree, G. Swapna, R. Yantri, R.J. Martis, L. Saba, G. Krishnamurthi, G. Mallarini, A.J. El-Baz, t, in: Reatment, Prostate Tissue Characterization/classification in 144 Patient Population Using Wavelet and Higher Order Spectra Features from Transrectal Ultrasound Images, vol. 12, 2013, pp. 545–557.

[118] U.R. Acharya, F. Molinari, S.V. Sree, G. Swapna, L. Saba, S. Guerriero, J.S. Suri, Treatment, Ovarian Tissue Characterization in Ultrasound: a Review, vol. 14, 2015, pp. 251–261.

[119] U.R. Acharya, S.V. Sree, S. Kulshreshtha, F. Molinari, J.E.W. Koh, L. Saba, J.S. Suri, Treatment, GyneScan: an Improved Online Paradigm for Screening of Ovarian Cancer via Tissue Characterization, vol. 13, 2014, pp. 529–539.

[120] V. Viswanathan, A.D. Jamthikar, D. Gupta, N. Shanu, A. Puvvula, N.N. Khanna, L. Saba, T. Omerzum, K. Viskovic, S.J.F.i.B. Mavrogeni, Low-cost Preventive Screening Using Carotid Ultrasound in Patients with Diabetes, vol. 25, 2020, pp. 1132–1171.

[121] U.R. Acharya, G. Swapna, S.V. Sree, F. Molinari, S. Gupta, R.H. Bardales, A. Witkowska, J.S. Suri, Treatment, A Review on Ultrasound-Based Thyroid Cancer Tissue Characterization and Automated Classification, vol. 13, 2014, pp. 289–301.

[122] V.K. Shrivastava, N.D. Londhe, R.S. Sonawane, J.S.J.C.m. Suri, p.i. Biomedicine, Computer-Aided Diagnosis of Psoriasis Skin Images with HOS, Texture and Color Features: a First Comparative Study of its Kind, vol. 126, 2016, pp. 98–109.

[123] V.K. Shrivastava, N.D. Londhe, R.S. Sonawane, J.S.J.C.m. Suri, p.i. biomedicine, A Novel and Robust Bayesian Approach for Segmentation of Psoriasis Lesions and its Risk Stratification, vol. 150, 2017, pp. 9–22.

[124] U.R. Acharya, K.P. Joseph, N. Kannathal, C.M. Lim, J.S.J.M. Suri, B. Engineering, Computing, Heart Rate Variability: a Review, vol. 44, 2006, pp. 1031–1051.

[125] G. Corrias, D. Cocco, J.S. Suri, L. Meloni, F. Cademartiri, L.J.C.D. Saba, Therapy, Heart applications of 4D flow 10 (2020) 1140.

[126] U.R. Acharya, S.V. Sree, M.M.R. Krishnan, N. Krishnananda, S. Ranjan, P. Umesh, J.S.J.C.m. Suri, p.i. Biomedicine, Automated Classification of Patients with Coronary Artery Disease Using Grayscale Features from Left Ventricle Echocardiographic Images, vol. 112, 2013, pp. 624–632.

[127] M. Maniruzzaman, M.J. Rahman, B. Ahammed, M.M. Abedin, H.S. Suri, M. Biswas, A. El-Baz, P. Bangeas, G. Tsoulfas, J.S.J.C.m. Suri, p.i. biomedicine, Statistical Characterization and Classification of Colon Microarray Gene Expression Data Using Multiple Machine Learning Paradigms, vol. 176, 2019, pp. 173–193.

[128] N.N. Khanna, A.D. Jamthikar, D. Gupta, M. Piga, L. Saba, C. Carcassi, A. A. Giannopoulos, A. Nicolaides, J.R. Laird, H.S.J. Suri, Rheumatoid Arthritis: Atherosclerosis Imaging and Cardiovascular Risk Assessment Using Machine and Deep Learning–Based Tissue Characterization, vol. 21, 2019, p. 7.

[129] J. Jiang, Y.C. Hu, N. Tyagi, P. Zhang, A. Rimner, J.O. Deasy, H. Veeraraghavan, Cross-modality (CT-MRI) prior augmented deep learning for robust lung tumor segmentation from small MR datasets, Med. Phys. 46 (2019) 4392–4404.

[130] G. Aresta, C. Jacobs, T. Araujo, A. Cunha, I. Ramos, B. van Ginneken, A. Campilho, iW-Net: an automatic and minimalistic interactive lung nodule segmentation deep network, Sci. Rep. 9 (2019) 11591.

[131] M. Anthimopoulos, S. Christodoulidis, L. Ebner, T. Geiser, A. Christe, S. Mougiakakou, Semantic segmentation of pathological lung tissue with dilated fully convolutional networks, IEEE J Biomed Health Inform 23 (2019) 714–722.

[132] T. Weikert, T. Akinci D'Antonoli, J. Bremerich, B. Stieltjes, G. Sommer, A. W. Sauter, Evaluation of an AI-powered lung nodule algorithm for detection and 3D segmentation of primary lung tumors, Contrast Media Mol. Imaging (2019) 1545747, 2019.

[133] H. Liu, H. Cao, E. Song, G. Ma, X. Xu, R. Jin, Y. Jin, C.C. Hung, A cascaded dual-pathway residual network for lung nodule segmentation in CT images, Phys. Med. 63 (2019) 112–121.

[134] N. Wong Yuzhen, S. Barrett, A review of automatic lung tumour segmentation in the era of 4DCT, Rep. Practical Oncol. Radiother. 24 (2019) 208–220.

[135] B. Park, H. Park, S.M. Lee, J.B. Seo, N. Kim, Lung segmentation on HRCT and volumetric CT for diffuse interstitial lung disease using deep convolutional neural networks, J. Digit. Imag. 32 (2019) 1019–1026.

[136] N. Nasrullah, J. Sang, M.S. Alam, M. Mateen, B. Cai, H. Hu, Automated lung nodule detection and classification using deep learning combined with multiple strategies, Sensors 19 (2019).

[137] M. Xu, S. Qi, Y. Yue, Y. Teng, L. Xu, Y. Yao, W. Qian, Segmentation of lung parenchyma in CT images using CNN trained with the clustering algorithm generated dataset, Biomed. Eng. Online 18 (2019) 2.

[138] S. Baek, Y. He, B.G. Allen, J.M. Buatti, B.J. Smith, L. Tong, Z. Sun, J. Wu, M. Diehn, B.W. Loo, K.A. Plichta, S.N. Seyedin, M. Gannon, K.R. Cabel, Y. Kim, X. Wu, Deep segmentation networks predict survival of non-small cell lung cancer, Sci. Rep. 9 (2019) 17286.

[139] T. Pang, S. Guo, X. Zhang, L. Zhao, Automatic lung segmentation based on texture and deep features of HRCT images with interstitial lung disease, BioMed Res. Int. (2019) 2045432, 2019.

[140] G. Chen, D. Xiang, B. Zhang, H. Tian, X. Yang, F. Shi, W. Zhu, B. Tian, X. Chen, Automatic pathological lung segmentation in low-dose CT image using eigenspace sparse shape composition, IEEE Trans. Med. Imag. 38 (2019) 1736–1749.

[141] K. Senthil Kumar, K. Venkatalakshmi, K. Karthikeyan, Lung cancer detection using image segmentation by means of various evolutionary algorithms, Comput Math Methods Med (2019) 4909846, 2019.

[142] C. Liu, R. Zhao, M. Pang, A fully automatic segmentation algorithm for CT lung images based on random forest, Med. Phys. 47 (2020) 518–529.

[143] L. Geng, S. Zhang, J. Tong, Z. Xiao, Lung segmentation method with dilated convolution based on VGG-16 network, Comput Assist Surg (Abingdon) 24 (2019) 27–33.

[144] A.M. Sousa, S.B. Martins, A.X. Falcao, F. Reis, E. Bagatin, K. Irion, ALTIS: a fast and automatic lung and trachea CT-image segmentation method, Med. Phys. 46 (2019) 4970–4982.

[145] J.C. Souza, J.O. Bandeira Diniz, J.L. Ferreira, G.L. Franca da Silva, A. Correa Silva, A.C. de Paiva, An automatic method for lung segmentation and reconstruction in chest X-ray using deep neural networks, Comput. Methods Progr. Biomed. 177 (2019) 285–296.

[146] N.M. Noor, J.C.M. Than, O.M. Rijal, R.M. Kassim, A. Yunus, A.A. Zeki, M. Anzidei, L. Saba, J.S. Suri, Automatic lung segmentation using control feedback system: morphology and texture paradigm, J. Med. Syst. 39 (2015).

[147] Q. Ni, Z.Y. Sun, L. Qi, W. Chen, Y. Yang, L. Wang, X. Zhang, L. Yang, Y. Fang, Z. Xing, Z. Zhou, Y. Yu, G.M. Lu, L.J. Zhang, A deep learning approach to characterize 2019 coronavirus disease (COVID-19) pneumonia in chest CT images, Eur. Radiol. 30 (2020) 6517–6527.

[148] F. Shan, Y. Gao, J. Wang, W. Shi, N. Shi, M. Han, Z. Xue, Y.J.a.p.a. Shi, Lung Infection Quantification of Covid-19 in Ct Images with Deep Learning, 2020.

[149] E.J. Hwang, H. Kim, S.H. Yoon, J.M. Goo, C.M. Park, Implementation of a deep learning-based computer-aided detection system for the interpretation of chest radiographs in patients suspected for COVID-19, Korean J. Radiol. 21 (2020) 1150–1160.

[150] S. Roy, W. Menapace, S. Oei, B. Luijten, E. Fini, C. Saltori, I. Huijben, N. Chennakeshava, F. Mento, A. Sentelli, E. Peschiera, R. Trevisan, G. Maschietto, E. Torri, R. Inchingolo, A. Smargiassi, G. Soldati, P. Rota, A. Passerini, R.J.G. van Sloun, E. Ricci, L. Demi, Deep learning for classification and localization of COVID-19 markers in point-of-care lung ultrasound, IEEE Trans. Med. Imag. 39 (2020) 2676–2687.

[151] A. Signoroni, M. Savardi, S. Benini, N. Adami, R. Leonardi, P. Gibellini, F. Vaccher, M. Ravanelli, A. Borghesi, R.J.a.p.a. Maroldi, End-to-end Learning for Semiquantitative Rating of COVID-19 Severity on Chest X-Rays, 2020.

[152] Z. Li, Z. Zhong, Y. Li, T. Zhang, L. Gao, D. Jin, Y. Sun, X. Ye, L. Yu, Z. Hu, J. Xiao, L. Huang, Y. Tang, From community-acquired pneumonia to COVID-19: a deep learning-based method for quantitative analysis of COVID-19 on thick-section CT scans, Eur. Radiol. 30 (2020) 6828–6837.

[153] S. Chaganti, P. Grenier, A. Balachandran, G. Chabin, S. Cohen, T. Flohr, B. Georgescu, S. Grbic, S. Liu, F. Mellot, N. Murray, S. Nicolaou, W. Parker, T. Re, P. Sanelli, A.W. Sauter, Z. Xu, Y. Yoo, V. Ziebandt, D. Comaniciu, Automated quantification of CT patterns associated with COVID-19 from chest CT, Radiology: Artif. Intell. 2 (2020), e200048.

[154] L. Li, L. Qin, Z. Xu, Y. Yin, X. Wang, B. Kong, J. Bai, Y. Lu, Z. Fang, Q. Song, K. Cao, D. Liu, G. Wang, Q. Xu, X. Fang, S. Zhang, J. Xia, J. Xia, Using artificial intelligence to detect COVID-19 and community-acquired pneumonia based on pulmonary CT: evaluation of the diagnostic accuracy, Radiology 296 (2020) E65–E71.

[155] S. Yang, L. Jiang, Z. Cao, L. Wang, J. Cao, R. Feng, Z. Zhang, X. Xue, Y. Shi, F. Shan, Deep learning for detecting corona virus disease 2019 (COVID-19) on high-resolution computed tomography: a pilot study, Ann. Transl. Med. 8 (2020), 450-450.

[156] S. Hu, Y. Gao, Z. Niu, Y. Jiang, L. Li, X. Xiao, M. Wang, E.F. Fang, W. Menpes-Smith, J. Xia, H. Ye, G. Yang, Weakly supervised deep learning for COVID-19

infection detection and classification from CT images, IEEE Access 8 (2020) 118869–118883.

[157] K. Zhang, X. Liu, J. Shen, Z. Li, Y. Sang, X. Wu, Y. Zha, W. Liang, C. Wang, K. Wang, L. Ye, M. Gao, Z. Zhou, L. Li, J. Wang, Z. Yang, H. Cai, J. Xu, L. Yang, W. Cai, W. Xu, S. Wu, W. Zhang, S. Jiang, L. Zheng, X. Zhang, L. Wang, L. Lu, J. Li, H. Yin, W. Wang, O. Li, C. Zhang, L. Liang, T. Wu, R. Deng, K. Wei, Y. Zhou, T. Chen, J.Y.-N. Lau, M. Fok, J. He, T. Lin, W. Li, G. Wang, Clinically applicable AI system for accurate diagnosis, quantitative measurements, and prognosis of COVID-19 pneumonia using computed tomography, Cell 181 (2020) 1423–1433, e1411.

[158] L. Carrer, E. Donini, D. Marinelli, M. Zanetti, F. Mento, E. Torri, A. Smargiassi, R. Inchingolo, G. Soldati, L. Demi, F. Bovolo, L. Bruzzone, Automatic pleural line extraction and COVID-19 scoring from lung ultrasound data, IEEE Trans. Ultrason. Ferroelectrics Freq. Contr. 67 (2020) 2207–2217.

[159] Z. Tang, W. Zhao, X. Xie, Z. Zhong, F. Shi, J. Liu, D.J.a.p.a. Shen, Severity Assessment of Coronavirus Disease 2019 (COVID-19) Using Quantitative Features from Chest CT Images, 2020.

[160] S. Rajaraman, J. Siegelman, P.O. Alderson, L.S. Folio, L.R. Folio, S.K. Antani, Iteratively pruned deep learning ensembles for COVID-19 detection in chest X-rays, IEEE Access 8 (2020) 115041–115050.

[161] J. Born, G. Brändle, M. Cossio, M. Disdier, J. Goulet, J. Roulin, N.J.a.p. a. Wiedemann, POCOVID-net: Automatic Detection of COVID-19 from a New Lung Ultrasound Imaging Dataset, POCUS, 2020.

[162] A. Jaiswal, N. Gianchandani, D. Singh, V. Kumar, M. Kaur, Classification of the COVID-19 infected patients using DenseNet201 based deep transfer learning, J. Biomol. Struct. Dyn. (2020) 1–8.

[163] N. Tsiknakis, E. Trivizakis, E.E. Vassalou, G.Z. Papadakis, D.A. Spandidos, A. Tsatsakis, J. Sánchez-García, R. López-González, N. Papanikolaou, A. H. Karantanas, K. Marias, Interpretable artificial intelligence framework for COVID-19 screening on chest X-rays, Exp Ther Med 20 (2020) 727–735.

[164] H.S. Maghdid, A.T. Asaad, K.Z. Ghafoor, A.S. Sadiq, M.K. Khan, Diagnosing COVID-19 Pneumonia from X-Ray and CT Images Using Deep Learning and Transfer Learning Algorithms, 2020.

[165] V.K. Shrivastava, N.D. Londhe, R.S. Sonawane, J.S. Suri, Computer-aided diagnosis of psoriasis skin images with HOS, texture and color features: a first comparative study of its kind, Comput. Methods Progr. Biomed. 126 (2016) 98–109.

[166] A. Chen, R.A. Karwoski, D.S. Gierada, B.J. Bartholmai, C.W. Koo, Quantitative CT analysis of diffuse lung disease, Radiographics 40 (2020) 28–43.

[167] J.C.M. Than, L. Saba, N.M. Noor, O.M. Rijal, R.M. Kassim, A. Yunus, H.S. Suri, M. Porcu, J.S. Suri, Lung disease stratification using amalgamation of Riesz and Gabor transforms in machine learning framework, Comput. Biol. Med. 89 (2017) 197–211.

[168] A. Hattori, K. Takamochi, S. Oh, K. Suzuki, New revisions and current issues in the eighth edition of the TNM classification for non-small cell lung cancer, Jpn. J. Clin. Oncol. 49 (2019) 3–11.

[169] T. Saba, Automated lung nodule detection and classification based on multiple classifiers voting, Microsc. Res. Tech. 82 (2019) 1601–1609.

[170] G. Zhang, Z. Yang, L. Gong, S. Jiang, L. Wang, Classification of benign and malignant lung nodules from CT images based on hybrid features, Phys. Med. Biol. 64 (2019) 125011.

[171] D. Singh, V. Kumar, Vaishali, M. Kaur, Classification of COVID-19 patients from chest CT images using multi-objective differential evolution-based convolutional neural networks, Eur. J. Clin. Microbiol. Infect. Dis. 39 (2020) 1379–1389.

[172] T. Mahmud, M.A. Rahman, S.A. Fattah, CovXNet: a multi-dilation convolutional neural network for automatic COVID-19 and other pneumonia detection from chest X-ray images with transferable multi-receptive feature optimization, Comput. Biol. Med. 122 (2020), 103869-103869.

[173] D. Das, K.C. Santosh, U. Pal, Truncated Inception Net: COVID-19 Outbreak Screening Using Chest X-Rays, Research Square, 2020.

[174] T. Ozturk, M. Talo, E.A. Yildirim, U.B. Baloglu, O. Yildirim, U. Rajendra Acharya, Automated detection of COVID-19 cases using deep neural networks with X-ray images, Comput. Biol. Med. 121 (2020), 103792-103792.

[175] L. Brunese, F. Mercaldo, A. Reginelli, A. Santone, Explainable deep learning for pulmonary disease and coronavirus COVID-19 detection from X-rays, Comput. Methods Progr. Biomed. 196 (2020) 105608.

[176] J.S. Suri, S. Singh, L.J.P.A. Reden, Applications, Fusion of Region and Boundary/surface-Based Computer Vision and Pattern Recognition Techniques for 2-D and 3-D MR Cerebral Cortical Segmentation (Part-II): A State-Of-The-Art Review, vol. 5, 2002, pp. 77–98.

[177] J.S. Suri, S. Singh, L.J.P.A. Reden, Applications, Computer vision and pattern recognition techniques for 2-D and 3-D MR cerebral cortical segmentation (Part I): a state-of-the-art review 5 (2002) 46–76.

[178] J.S. Suri, K. Liu, L. Reden, S.J. Laxminarayan, B. Society, A review on MR vascular image processing: skeleton versus nonskeleton approaches: part II 6 (2002) 338.

[179] https://xmedcon.sourceforge.io/.

[180] S.P. Sahu, B. Kamble, R. Doriya, 3D Lung Segmentation Using Thresholding and Active Contour Method, Advances in Intelligent Systems and Computing, Springer Singapore, 2020, pp. 369–380.

[181] M.E. Taylor, Transfer between Different Reinforcement Learning Methods, Transfer in Reinforcement Learning Domains, Springer Berlin Heidelberg, 2009, pp. 139–179.

[182] U.R. Acharya, G. Swapna, S.V. Sree, F. Molinari, S. Gupta, R.H. Bardales, A. Witkowska, J.S. Suri, A review on ultrasound-based thyroid cancer tissue characterization and automated classification, Technol. Canc. Res. Treat. 13 (2014) 289–301.

[183] A.R. Shih, H. Uruga, E. Bozkurtlar, J.H. Chung, L.P. Hariri, Y. Minami, H. Wang, A. Yoshizawa, A. Muzikansky, A.L. Moreira, M. Mino-Kenudson, Problems in the reproducibility of classification of small lung adenocarcinoma: an international interobserver study, Histopathology 75 (2019) 649–659.

[184] A. LeNail, Nn-SVG: Publication-ready neural network architecture schematics, J Open Source Software 4 (2019) 747.

[185] H. Iqbal, HarisIqbal88/PlotNeuralNet v1.0.0, 2018.

[186] F. Ye, J. Pu, J. Wang, Y. Li, H. Zha, Glioma grading based on 3D multimodal convolutional neural network and privileged learning, in: 2017 IEEE International Conference on Bioinformatics and Biomedicine (BIBM), IEEE, 2017.

[187] S. Wang, Y. Zha, W. Li, Q. Wu, X. Li, M. Niu, M. Wang, X. Qiu, H. Li, H. Yu, W. Gong, Y. Bai, L. Li, Y. Zhu, L. Wang, J. Tian, A fully automatic deep learning system for COVID-19 diagnostic and prognostic analysis, Eur. Respir. J. 56 (2020).

[188] S.H. Yoo, H. Geng, T.L. Chiu, S.K. Yu, D.C. Cho, J. Heo, M.S. Choi, I.H. Choi, C. Cung Van, N.V. Nhung, B.J. Min, H. Lee, Deep learning-based decision-tree classifier for COVID-19 diagnosis from chest X-ray imaging, Front. Med. 7 (2020) 427.

[189] J. Zhu, B. Shen, A. Abbasi, M. Hoshmand-Kochi, H. Li, T.Q. Duong, Deep transfer learning artificial intelligence accurately stages COVID-19 lung disease severity on portable chest radiographs, PLoS One 15 (2020), e0236621.

[190] Guidance Statement by the American College of Radiology.

[191] H. Yasar, M. Ceylan, A novel comparative study for detection of Covid-19 on CT lung images using texture analysis, machine learning, and deep learning methods, Multimed. Tool. Appl. (2020) 1–25.

[192] L. Setti, M. Kirienko, S.C. Dalto, M. Bonacina, E. Bombardieri, FDG-PET/CT findings highly suspicious for COVID-19 in an Italian case series of asymptomatic patients, Eur. J. Nucl. Med. Mol. Imag. 47 (2020) 1649–1656.

[193] J. Alonso Sanchez, J. García Prieto, A. Galiana Morón, J.P. Pilkington-Woll, PET/CT of COVID-19 as an organizing pneumonia, Clin. Nucl. Med. 45 (2020) 642–643.

[194] J. Castanheira, A. Mascarenhas Gaivão, S. Mairos Teixeira, P.J. Pereira, D. C. Costa, Asymptomatic COVID-19 positive patient suspected on FDG-PET/CT, Nucl. Med. Commun. 41 (2020) 598–599.

[195] J.P. Cohen, L. Dao, K. Roth, P. Morrison, Y. Bengio, A.F. Abbasi, B. Shen, H. K. Mahsa, M. Ghassemi, H. Li, T. Duong, Predicting COVID-19 pneumonia severity on chest X-ray with deep learning, Cureus (2020).

[196] M.K. Galougahi, J. Ghorbani, M. Bakhshayeshkaram, A.S. Naeini, S.J.A.R. Haseli, Olfactory Bulb Magnetic Resonance Imaging in SARS-CoV-2-Induced Anosmia: the First Report, 2020.

[197] H. Gunraj, L. Wang, A.J.a.p.a. Wong, Covidnet-ct: A Tailored Deep Convolutional Neural Network Design for Detection of Covid-19 Cases from Chest Ct Images, 2020.

[198] A.M. Ismael, A. Sengur, Deep learning approaches for COVID-19 detection based on chest X-ray images, Expert Syst. Appl. 164 (2021) 114054.

[199] S.G. Kandemirli, L. Dogan, Z.T. Sarikaya, S. Kara, C. Akinci, D. Kaya, Y. Kaya, D. Yildirim, F. Tuzuner, M.S. Yildirim, E. Ozluk, B. Gucyetmez, E. Karaarslan, I. Koyluoglu, H.S. Demirel Kaya, O. Mammadov, I. Kisa Ozdemir, N. Afsar, B. Citci Yalcinkaya, S. Rasimoglu, D.E. Guduk, A. Kedir Jima, A. Ilksoz, V. Ersoz, M. Yonca Eren, N. Celtik, S. Arslan, B. Korkmazer, S.S. Dincer, E. Gulek, I. Dikmen, M. Yazici, S. Unsal, T. Ljama, I. Demirel, A. Ayyildiz, I. Kesimci, S. Bolsoy Deveci, M. Tutuncu, O. Kizilkilic, L. Telci, R. Zengin, A. Dincer, I. O. Akinci, N. Kocer, Brain MRI findings in patients in the intensive care unit with COVID-19 infection, Radiology 297 (2020) E232–e235.

[200] F. Kay, S. Abbara, The Many Faces of COVID-19: Spectrum of Imaging Manifestations, Radiological Society of North America, 2020.

[201] G. Litjens, T. Kooi, B.E. Bejnordi, A.A.A. Setio, F. Ciompi, M. Ghafoorian, J.A.W. M. van der Laak, B. van Ginneken, C.I. Sánchez, A survey on deep learning in medical image analysis, Med. Image Anal. 42 (2017) 60–88.

[202] S. Minaee, R. Kafieh, M. Sonka, S. Yazdani, G. Jamalipour Soufi, Deep-COVID: predicting COVID-19 from chest X-ray images using deep transfer learning, Med. Image Anal. 65 (2020) 101794.

[203] F. Shi, L. Xia, F. Shan, D. Wu, Y. Wei, H. Yuan, H. Jiang, Y. Gao, H. Sui, D.J.a.p. a. Shen, Large-scale Screening of Covid-19 from Community Acquired Pneumonia Using Infection Size-Aware Classification, 2020.

[204] H. Panwar, P.K. Gupta, M.K. Siddiqui, R. Morales-Menendez, P. Bhardwaj, V. Singh, A deep learning and grad-CAM based color visualization approach for fast detection of COVID-19 cases using chest X-ray and CT-Scan images, Chaos, Solit. Fractals 140 (2020), 110190-110190.

[205] C. Ouchicha, O. Ammor, M. Meknassi, CVDNet: a novel deep learning architecture for detection of coronavirus (Covid-19) from chest x-ray images, Chaos, Solit. Fractals 140 (2020), 110245-110245.

[206] M. Farooq, A.J.a.p.a. Hafeez, Covid-resnet: A Deep Learning Framework for Screening of Covid19 from Radiographs, 2020.

[207] D. Cozzi, M. Albanesi, E. Cavigli, C. Moroni, A. Bindi, S. Luvarà, S. Lucarini, S. Busoni, L.N. Mazzoni, V. Miele, Chest X-ray in new Coronavirus Disease 2019 (COVID-19) infection: findings and correlation with clinical outcome, Radiol. Med. 125 (2020) 730–737.

[208] R.M. Pereira, D. Bertolini, L.O. Teixeira, C.N. Silla Jr., Y.M.G. Costa, COVID-19 identification in chest X-ray images on flat and hierarchical classification scenarios, Comput. Methods Progr. Biomed. 194 (2020), 105532-105532.

[209] A.A. Ardakani, A.R. Kanafi, U.R. Acharya, N. Khadem, A. Mohammadi, Application of deep learning technique to manage COVID-19 in routine clinical practice using CT images: results of 10 convolutional neural networks, Comput. Biol. Med. 121 (2020), 103795-103795.

[210] C. Zheng, X. Deng, Q. Fu, Q. Zhou, J. Feng, H. Ma, W. Liu, X. Wang, Deep Learning-Based Detection for COVID-19 from Chest CT Using Weak Label, Cold Spring Harbor Laboratory, 2020.

[211] X. Yang, X. He, J. Zhao, Y. Zhang, S. Zhang, P.J.A.e.-p. Xie, Covid-CT-dataset: A CT Scan Dataset about Covid-19, 2020 arXiv: 2003.13865.

[212] O. Gozes, M. Frid-Adar, N. Sagie, A. Kabakovitch, D. Amran, R. Amer, H. Greenspan, A Weakly Supervised Deep Learning Framework for COVID-19 CT Detection and Analysis, Thoracic Image Analysis, Springer International Publishing, 2020, pp. 84–93.

[213] B. Liu, X. Gao, M. He, L. Liu, G. Yin, A fast online COVID-19 diagnostic system with chest CT scans, Proc KDD 2020 (2020).

[214] E.E.-D. Hemdan, M.A. Shouman, M.E. Karar, Covidx-net: A Framework of Deep Learning Classifiers to Diagnose Covid-19 in X-Ray Images, 2020.

[215] J. Zhang, Y. Xie, Z. Liao, G. Pang, J. Verjans, W. Li, Z. Sun, J. He, C.S. Yi Li, Viral Pneumonia Screening on Chest X-Ray Images Using Confidence-Aware Anomaly Detection, 2020.

[216] N. Narayan Das, N. Kumar, M. Kaur, V. Kumar, D. Singh, Automated deep transfer learning-based approach for detection of COVID-19 infection in chest X-rays, Ing Rech Biomed (2020), https://doi.org/10.1016/j.irbm.2020.1007.1001.

[217] Y.-H. Wu, S.-H. Gao, J. Mei, J. Xu, D.-P. Fan, C.-W. Zhao, M. Cheng, JCS: an Explainable COVID-19 Diagnosis System by Joint Classification and Segmentation, 2020.

[218] M. Toğaçar, B. Ergen, Z. Cömert, COVID-19 detection using deep learning models to exploit Social Mimic Optimization and structured chest X-ray images using fuzzy color and stacking approaches, Comput. Biol. Med. 121 (2020), 103805-103805.

[219] S. Basu, S.J.a.p.a. Mitra, Deep Learning for Screening COVID-19 Using Chest X-Ray Images, 2020.

[220] O. Gozes, M. Frid-Adar, H. Greenspan, P.D. Browning, H. Zhang, W. Ji, A. Bernheim, E.J.a.p.a. Siegel, Rapid Ai Development Cycle for the Coronavirus (Covid-19) Pandemic: Initial Results for Automated Detection & Patient Monitoring Using Deep Learning Ct Image Analysis, 2020.

[221] T. Yan, P.K. Wong, H. Ren, H. Wang, J. Wang, Y.J.C. Li, Solitons, Fractals, Automatic distinction between covid-19 and common pneumonia using multi-scale convolutional neural network on chest ct scans 140 (2020) 110153.

[222] Y. Oh, S. Park, J.C. Ye, Deep Learning Covid-19 Features on Cxr Using Limited Training Data Sets, 2020.

[223] L. Saba, J.C.M. Than, N.M. Noor, O.M. Rijal, R.M. Kassim, A. Yunus, C.R. Ng, J. S. Suri, Inter-observer variability analysis of automatic lung delineation in normal and disease patients, J. Med. Syst. 40 (2016).

[224] K. Liu, J.S. Suri, Automatic Vessel Indentification for Angiographic Screening, Google Patents, 2005.

[225] B. Ambale-Venkatesh, X. Yang, C.O. Wu, K. Liu, W.G. Hundley, R. McClelland, A. S. Gomes, A.R. Folsom, S. Shea, E. Guallar, D.A. Bluemke, J.A.C. Lima, Cardiovascular event prediction by machine learning: the multi-ethnic study of atherosclerosis, Circ. Res. 121 (2017) 1092–1101.

[226] G.S. Tandel, A. Balestrieri, T. Jujaray, N.N. Khanna, L. Saba, J.S. Suri, Multiclass magnetic resonance imaging brain tumor classification using artificial intelligence paradigm, Comput. Biol. Med. 122 (2020) 103804.

[227] V.K. Shrivastava, N.D. Londhe, R.S. Sonawane, J.S. Suri, A novel and robust Bayesian approach for segmentation of psoriasis lesions and its risk stratification, Comput. Methods Progr. Biomed. 150 (2017) 9–22.

[228] A. Jamthikar, D. Gupta, L. Saba, N.N. Khanna, K. Viskovic, S. Mavrogeni, J. R. Laird, N. Sattar, A.M. Johri, G.J.C.i.B. Pareek, Medicine, Artificial Intelligence Framework for Predictive Cardiovascular and Stroke Risk Assessment Models: A Narrative Review of Integrated Approaches Using Carotid Ultrasound, 2020, p. 104043.

[229] X. Wu, H. Hui, M. Niu, L. Li, L. Wang, B. He, X. Yang, L. Li, H. Li, J. Tian, Y. Zha, Deep learning-based multi-view fusion model for screening 2019 novel coronavirus pneumonia: a multicentre study, Eur. J. Radiol. 128 (2020), 109041-109041.

[230] W.H. Organization, Use of Chest Imaging in COVID-19, 2020, pp. 1–56.

[231] G.T. Yusuf, A. Wong, D. Rao, A. Tee, C. Fang, P.S. Sidhu, The use of contrast-enhanced ultrasound in COVID-19 lung imaging, J Ultrasound (2020) 1–5.

[232] Q. Ni, Z.Y. Sun, L. Qi, W. Chen, Y. Yang, L. Wang, X. Zhang, L. Yang, Y. Fang, Z.J. E.r. Xing, A Deep Learning Approach to Characterize 2019 Coronavirus Disease (COVID-19) Pneumonia in Chest CT Images, vol. 30, 2020, pp. 6517–6527.

[233] S. Wang, Y. Zha, W. Li, Q. Wu, X. Li, M. Niu, M. Wang, X. Qiu, H. Li, H.J.E.R.J. Yu, A Fully Automatic Deep Learning System for COVID-19 Diagnostic and Prognostic Analysis, 2020.

[234] R. Narayanan, P.N. Werahera, A. Barqawi, E.D. Crawford, K. Shinohara, A. R. Simoneau, J.S. Suri, Adaptation of a 3D prostate cancer atlas for transrectal ultrasound guided target-specific biopsy, Phys. Med. Biol. 53 (2008) N397–N406.

[235] F. Shen, R. Narayanan, J.S. Suri, Rapid motion compensation for prostate biopsy using GPU, in: Annual International Conference of the IEEE Engineering in Medicine and Biology Society. IEEE Engineering in Medicine and Biology Society. Annual International Conference, 2008, pp. 3257–3260, 2008.

[236] State of the Art in Neural Networks and Their Applications - 1st Edition.

[237] U.R. Acharya, S. Vinitha Sree, M.R. Mookiah, R. Yantri, F. Molinari, W. Zieleźnik, J. Małyszek-Tumidajewicz, B. Stępień, R.H. Bardales, A. Witkowska, J.S. Suri, Diagnosis of Hashimoto's thyroiditis in ultrasound using tissue characterization and pixel classification, Proc. IME H J. Eng. Med. 227 (2013) 788–798.

[238] S.G. Kandemirli, A. Altundag, D. Yildirim, D.E. Tekcan Sanli, O. Saatci, Olfactory bulb MRI and paranasal sinus CT findings in persistent COVID-19 anosmia, Acad. Radiol. 28 (1) (2020) 28–35.

[239] E. Cuadrado-Godia, P. Dwivedi, S. Sharma, A.O. Santiago, J.R. Gonzalez, M. Balcells, J. Laird, M. Turk, H.S. Suri, A.J.J.o.s. Nicolaides, Cerebral Small Vessel Disease: a Review Focusing on Pathophysiology, Biomarkers, and Machine Learning Strategies, vol. 20, 2018, p. 302.

[240] M. Maniruzzaman, N. Kumar, M.M. Abedin, M.S. Islam, H.S. Suri, A.S. El-Baz, J. S. J.C.m. Suri, p.i. biomedicine, Comparative Approaches for Classification of Diabetes Mellitus Data: Machine Learning Paradigm, vol. 152, 2017, pp. 23–34.

[241] R. Acharya, Y.E. Ng, J.S. Suri, Image Modeling of the Human Eye, Artech House, 2008.

[242] A. El-Baz, J. Suri, Lung Imaging and CADx, CRC Press, 2019.

[243] A. El-Baz, J.S. Suri, Lung Imaging and Computer Aided Diagnosis, CRC Press, 2011.

[244] Online COVID-19 Diagnosis with Chest CT Images: Lesion-Attention Deep Neural Networks, Rescognito, Inc.

Symbol Table

2-D: Two dimensions
3-D: Three dimensions
ACC: Accuracy
AI: Artificial intelligence
ARDS: Acute respiratory distress syndrome
AUC: Area-under-the-curve
CNN: Convolution neural network
CT: Computed tomography
DL: Deep learning
FS: F1-score
GPU: Graphics Processing Unit
H/W and S/W: Hardware and software
LUS: Lung ultrasound
ML: Machine learning
MRI: Magnetic resonance imaging
RF: Random forest
RSNA: Radiological Society of North America
SE: Sensitivity
SP: Specificity
TL: Transfer learning
US: Ultrasound
X-ray: Röntgen radiation